Cardiac-Specific YAP Activation Improves Cardiac Function and Survival in an Experimental Murine Myocardial Infarction Model

Zhiqiang Lin, Alexander von Gise, Pingzhu Zhou, Fei Gu, Qing Ma, Jiangming Jiang, Allan L Yau, Jessica N Buck, Katryna A Gouin, Pim R van Gorp, Bin Zhou, Jinghai Chen, Jon G Seidman, Da-Zhi Wang and William T Pu

Circ Res. published online May 15, 2014;
Circulation Research is published by the American Heart Association, 7272 Greenville Avenue, Dallas, TX 75231

Print ISSN: 0009-7330. Online ISSN: 1524-4571

Cardiac-Specific YAP Activation Improves Cardiac Function and Survival in an Experimental Murine Myocardial Infarction Model

Zhiqiang Lin[1], Alexander von Gise[1], Pingzhu Zhou[1], Fei Gu[1], Qing Ma[1], Jiangming Jiang[2], Allan L. Yau[1], Jessica N. Buck[1], Katryna A. Gouin[1], Pim R. R. van Gorp[1,3], Bin Zhou[1,5], Jinghai Chen[1], Jonathan G. Seidman[2], Da-zhi Wang[1,4] and William T. Pu[1,4,5]

[1]Department of Cardiology, Children's Hospital Boston, Harvard Medical School; [2]Department of Genetics, Harvard Medical School; [3]Department of Cardiology, Leiden University Medical Center; [4]Harvard Stem Cell Institute, Harvard University, and; [5]Key Laboratory of Nutrition and Metabolism, Institute for Nutritional Sciences, Shanghai Institutes for Biological Sciences, Chinese Academy of Sciences, Shanghai 200031, China.

Z.L., and A.v.G. contributed equally to this study.

Running title: YAP Enhances Outcome and CM Proliferation after MI

Subject codes:
[154] Myogenesis
[88] Gene therapy
[148] Heart failure-basic studies

Address correspondence to:
Dr. William T. Pu
Department of Cardiology
Children's Hospital Boston
Enders 1254
300 Longwood Ave.
Boston, MA 02115
Tel: 617-919-2091
Fax: 617-730-0140
wpu@enders.tch.harvard.edu

In April 2014, the average time from submission to first decision for all original research papers submitted to *Circulation Research* was 14.38 days.

DOI: 10.1161/CIRCRESAHA.115.303632

ABSTRACT

Rationale: Yes-Associated Protein (YAP), the terminal effector of the Hippo signaling pathway, is crucial for regulating embryonic cardiomyocyte (CM) proliferation.

Objective: We hypothesized that YAP activation after myocardial infarction would preserve cardiac function and improve survival.

Methods and Results: We used a cardiac-specific, inducible expression system to activate YAP in adult mouse heart. Activation of YAP in adult heart promoted CM proliferation and did not deleteriously affect heart function. Furthermore, YAP activation after myocardial infarction (MI) preserved heart function and reduced infarct size. Using adeno-associated virus subtype 9 (AAV9) as a delivery vector, we expressed human YAP in the adult murine myocardium immediately after MI. We found that AAV9:hYAP significantly improved cardiac function and mouse survival. AAV9:hYAP did not exert its salutary effects by reducing CM apoptosis. Rather, AAV9:hYAP stimulated adult CM proliferation. Gene expression profiling indicated that AAV9:hYAP stimulated expression of cell cycle genes and promoted a less mature cardiac gene expression signature.

Conclusions: Cardiac specific YAP activation after MI mitigated myocardial injury, improved cardiac function, and enhanced survival. These findings suggest that therapeutic activation of YAP or its downstream targets, potentially through AAV-mediated gene therapy, may be a strategy to improve outcome after MI.

Keywords:
YAP, myocardial infarction, AAV9, heart failure, survival, regeneration

Nonstandard Abbreviations and Acronyms:

MI	myocardial infarction
CM	cardiomyocyte
AAV9	adeno-associated virus serotype 9
AAV9:Luci	AAV9 with luciferase expressed from the cardiac troponin T promoter
AAV9:YAP	AAV9 with human YAP[S127A] expressed from the cardiac troponin T promoter
EdU	5-ethynyl-2'-deoxyuridine
YAP^{GOF}	Yap gain of function mice (genotype Myh6-Cre; $Rosa26^{fs.rtTA/fs.rtTA}$; TRE-YAP)
Dox	doxycycline
rtTA	reverse tetracycline activator protein
CFP	cyan fluorescent protein
GFP	green fluorescent protein
YFP	yellow fluorescent protein
RFP	red fluorescent protein
pH3	phosphohistone H3
MRI	magnetic resonance imaging
TUNEL	Terminal deoxynucleotidyl transferase dUTP nick end labeling

INTRODUCTION

Myocardial infarction causes the loss of billions of cardiomyocytes (CMs). Morbidity and mortality following myocardial infarction remain high despite modern medical and surgical management. The fundamental barrier to improving outcome is our inability to replace the lost CMs. To overcome this barrier, there has been tremendous interest in strategies to increase CM number by stimulating CM cell cycle re-entry, CM survival by inhibition of apoptosis, or CM differentiation from stem cells.

The Hippo-YAP pathway, originally identified in Drosophila as an important regulator of tissue growth[1], has attracted recent interest as a potential means to enhance heart regeneration. In this highly conserved signaling pathway, YAP, a transcriptional co-activator promotes organ growth and cellular proliferation by binding to sequence-specific transcription factors, most notably TEAD1[2], thereby activating expression of cell cycle regulators and other target genes. YAP expression and activity are tightly controlled, as excessive YAP activity causes tissue overgrowth and cancer, while insufficient YAP activity causes tissue hypoplasia[1]. The Hippo kinase cascade restrains YAP activity by catalyzing its phosphorylation on serine 127, which leads to its exclusion from the nucleus. Activation of YAP activity, either by inactivation of Hippo kinase cascade components,[3] or by forced expression of activated YAP lacking the Hippo kinase phosphorylation site,[4, 5] drives fetal CM proliferation, resulting in remarkable fetal overgrowth. On the other hand, cardiac-specific YAP deletion causes lethal cardiac hypoplasia.[4, 5] Thus, YAP is a potent stimulator of fetal CM proliferation.

In this study, we tested the hypothesis that adult stage, cardiac-specific activation of YAP drives CM proliferation and improves outcome in myocardial infarction. We found that long-term YAP activation did not cause cardiac hypertrophy. Transgenic or AAV9-mediated activation of YAP improved the heart function and survival after myocardial infarction (MI). These data show that cardiac-specific activation of YAP mitigates the injury caused by myocardial infarction, and suggest that therapeutic activation of YAP or its downstream targets may be a strategy to improve outcome after MI.

METHODS

Detailed Materials and Methods are provided in the Online Supplement. All animal procedures were approved by the Institutional Animal Care and Use Committee. MI, echocardiography, and MRI were performed and analyzed blinded to genotype and treatment group. Antibodies and primers used are listed in Online Tables I and II. 5-ethynyl-2'-deoxyuridine (EdU) was detected with the Click-iT EdU imaging kit (Invitrogen). AAV9 was prepared as described[6].

Values are expressed as mean ± SEM. Student's t-test and ANOVA with the Tukey HSD post-hoc test were used to test for statistical significance.

RESULTS

Inducible CM-specific YAP expression model,

We generated Myh6-Cre; ROSA26$^{fs.rtTA/fs.rtTA}$; TRE-YAP mice (referred to as YAP^{GOF}), which express activated human YAP selectively in CMs under the control of doxycycline (Dox) (Fig. 1A). The activated YAP protein contains the S127A mutation that inhibits its cytoplasmic sequestration by Hippo kinase

phosphorylation. We used Myh6-Cre; ROSA26$^{fs.rtTA/fs.rtTA}$ lacking TRE-YAP as controls. To validate transgene expression in YAP^{GOF} mice, we treated adult mice with Dox for four weeks and then analyzed YAP expression by western blotting (Fig. 1B-D). Compared to controls, YAP^{GOF} mice expressed elevated YAP in the heart but not in other organs (Fig. 1B-C). Moreover, YAP expression was dependent upon Dox administration (Fig. 1D).

YAP stimulates adult CM cell cycle activity in vivo.

Dox treatment from week of life 4 to 8 did not significantly change the size of YAP^{GOF} hearts compared with their littermate controls (Fig. 2A). At the same time, CM size was reduced (Fig. 2B-C), suggesting that YAP^{GOF} hearts contained more CMs (Fig 2D). We confirmed this finding by using collagenase perfusion to count dissociated CMs (Fig. 2E). Morphometry on dissociated, rod-shaped CMs confirmed smaller average CM size in YAP^{GOF} compared to control (Fig. 2F). We observed no change in sarcomere organization (Online Figure I), indicating that reduced CM size is not due to de-differentiation. The measured CM number was higher in YAP^{GOF} compared to control (Fig. 2G).

Increased CM number in hearts after adult stage YAP induction suggested that YAP stimulated CM cell cycle re-entry. We further tested this hypothesis by assessing CM proliferation after 4 weeks of YAP activation with two independent markers: phosphorylated histone H3 (pH3), an M phase marker; and EdU uptake, an S phase marker. In histological sections, the fraction of CMs positive for EdU or pH3 was respectively 4-fold and 5-fold higher in YAP^{GOF} compared to controls (Online Figure II). To further confirm this finding and exclude potential artifacts related to difficulty in establishing CM boundaries in tissue sections, we repeated these measurements in dissociated CM preparations. These studies confirmed that a significantly higher fraction of CMs were labeled by EdU or pH3 in YAP^{GOF} mice (Fig. 2G-H). YAP significantly increased the mononuclear CM fraction (YAP^{GOF}, 12.4% versus control, 7.1%), and EdU^{+} CMs were nearly exclusively mononuclear (Fig. 2I). This observation is consistent with other reports that proliferating CMs are more likely to be mononuclear.[7]

In vivo clonal assay demonstrates YAP stimulates productive CM cell cycle activity.

Numerous technical factors complicate measurement of CM proliferation in the adult heart,[8] including DNA synthesis in the absence of nuclear or cellular division (leading to polyploidy), nuclear division in the absence of cellular division (leading to multinucleation), and the infrequency of CM compared to non-myocyte proliferation. To provide further independent evidence that activated YAP stimulates CM cell cycle activity that generates new CMs, we used an in vivo clonal analysis strategy (Fig. 3A) similar to that recently used to demonstrate adult CM proliferation downstream of neuregulin.[7] In Myh6-MerCreMer; Rosa26$^{fs.rtTA/+}$; TRE-YAP; CAG-fs-RFP mice, low dose tamoxifen treatment induced irreversible RFP labeling and expression of the Dox-dependent reverse Tet activator protein (rtTA) in a small fraction of CMs (Online Figure III). Dox treatment selectively activated YAP expression in RFP-labeled CMs in the experimental group containing the TRE-YAP transgene, but not in controls lacking this transgene. If YAP stimulated CM proliferation and new myocyte formation, then we expected to find clusters containing two or more RFP^{+} CMs more frequently in the presence of the TRE-YAP transgene. Indeed, after 4 weeks on Dox the number of RFP^{+} clusters containing two or more labeled CMs was significantly greater in the aYAP expressing hearts (Fig. 3B-C), indicative of CM proliferation.

Chance labeling of adjacent CMs by independent Cre recombination events in this single color assay leads to a background of clusters with two or more cells that are not due to proliferation. To better account for these events, we refined the assay using a multi-color Cre reporter[9] (Fig. 3D-F), where each Cre recombination event triggers expression of one of four fluorescent reporters: cyan fluorescent protein (CFP), RFP, nuclear GFP (nGFP), and YFP. We had difficulty detecting endogenous fluorescence of CFP above autofluorescent background, and nGFP is only visible in cells when the plane of section goes through the

nucleus. Therefore we only considered RFP and YFP readouts. We classified clusters of cells as monochromatic or bichromatic (red and yellow arrows, respectively, Fig. 3E). Bichromatic clusters of two or more cells involved multiple recombination events rather than proliferation. These clusters occurred at similar frequency in YAP^{GOF} and control. In contrast, monochromatic clusters of two or more CMs potentially arose from proliferation. These clusters were more common in YAP^{GOF} (Fig. 3F), consistent with YAP stimulation of formation of new CMs through proliferation. This assay may underestimate the extent of YAP-driven CM proliferation, because it is likely that not all labeled CMs expressed YAP, and because random adjacent recombination continues to contribute to a subset of multicell clusters, increasing the baseline number of 2-cell clusters. Overall, the clonal assays supported the conclusion that aYAP stimulated productive CM cell cycle activity in the adult heart, and indicated that YAP action is cell autonomous.

Long-term induction of YAP did not cause cardiac hypertrophy.

Long-term YAP ectopic activation in the liver caused liver tumors[10, 11]. To test whether long-term YAP activation is deleterious to the heart, we overexpressed YAP in the heart by treating YAP^{GOF} mice with Dox for 4.5 months. Long-term YAP overexpression did not cause cardiac hypertrophy, as indicated by the heart size, heart-to-body weight ratio and left ventricle wall thickness (Fig. 4A-C). Echocardiography showed that heart function of YAP^{GOF} mice was similar to their control littermate at 2 and 3 months of Dox induction, but at 4 months, heart function was slightly lower in YAP^{GOF} than controls. The left ventricle wall thickness of control and YAP^{GOF} mice was similar even after 4 months of YAP activation (Fig. 4D). One month of YAP activation did not cause measureable cardiac fibrosis, while four months of YAP activation was accompanied by a slight, statistically significant increase in myocardial fibrosis (Fig. 4E-F). While YAP is an oncogene, no tumors were observed in YAP^{GOF} mice. These results indicate that long-term YAP overexpression did not cause cardiac hypertrophy and that YAP activation is well tolerated in the heart for at least 3 months. YAP activation for greater than three months may have deleterious effects (fibrosis; mild reduction of heart function) that would need to be balanced against potential benefits.

Cardiac specific expression of activated YAP mitigated myocardial injury.

YAP stimulation of CM proliferation, and the tolerance of the heart to sustained YAP activation, prompted us to ask whether YAP activation after myocardial infarction (MI) is beneficial. We designed our experiment to start hYAP induction one week after permanent LAD ligation (Fig. 5A), as it is likely that the major events in the immediate period after MI relate to cell death and we sought to focus on the pro-proliferative activity of YAP. We permanently ligated the left anterior descending coronary artery in 8-week-old control and YAP^{GOF} mice to induce MI. We then started Dox one week after surgery and continued it for four more weeks. At the end of the study, we measured heart function by cardiac magnetic resonance imaging (MRI), and then measured heart and body weight. The hearts were collected for histological analysis. The MRI data showed higher ejection fraction (EF%) in the YAP^{GOF} group compared to controls (Fig. 5B-C), indicating that YAP activation post-MI improves cardiac function. After MI, the heart typically undergoes hypertrophic remodeling to compensate for lost CMs, resulting in a higher heart to body weight ratio. In the long run, this cardiac hypertrophy is detrimental for cardiac function. We found that one month of YAP activation decreased heart to body weight ratio (Fig. 5D), suggesting that YAP activation attenuates hypertrophic remolding post MI. We visualized the myocardial scar in picro-sirius red/fast green-stained cryosections, where fibrotic tissue stains red and viable myocardium stains green (Fig. 5E)[12]. Compared with control mice, YAP^{GOF} mice had smaller infarct size, and this was confirmed by quantitative analysis (Fig. 5F). These data together suggest that activation of YAP after MI improved heart function and reduced infarct size.

To investigate the mechanisms underlying the beneficial activity of YAP, we measured CM apoptosis and proliferation in the post-MI hearts. At this time point five weeks after the MI, we did not detect

significant apoptosis of CM by TUNEL staining in remote, infarct or border zones, although we did find many $TUNEL^+$ non-myocytes. In contrast, the fraction of CMs labeled by EdU (administered twice over the 4^{th} post-MI week) or pH3 was higher in YAP^{GOF} compared to control in the tissue border and remote from the infarct (Fig. 5G-H). These results indicate that YAP stimulates post-MI CM proliferation, leading to reduced infarct size and improved myocardial outcome after MI.

Adenovirus associated virus subtype 9 delivery of hYAP.

Since cardiac-specific transgenic YAP activation appeared promising, we moved forward to test the potential of YAP gene therapy for improving myocardial outcome after MI. Adeno-associated virus (AAV) is a safe and efficient vector for in vivo gene transfer[13], and serotype 9 is significantly cardiotropic[14]. We generated AAV9:cTNT::3Flag-hYAP (AAV9:hYAP), in which the CM-specific chicken troponin T promoter drives expression of triply Flag-tagged, activated human YAP[S127A] (Online Figure IV-A). As a control, we generated AAV9:cTNT::Luciferase (AAV9:Luci), in which 3Flag-hYAP was replaced by luciferase.

We validated performance of the viral vectors by delivering them subcutaneously to 3-5 day old neonatal mice. Uninjected wild type neonatal mice were used as controls in these validation studies. Seven days after virus injection, hearts were analyzed analysis by western blotting and immunohistochemistry. Western blots showed a single endogenous YAP band in control mice, and an additional band in AAV9:hYAP-treated mice, reflecting the larger, exogenous 3Flag-hYAP (Online Figure IV-B). The luciferase protein was detected in hearts treated with AAV9:Luci but not in control hearts (Online Figure IV-C). Immunofluorescence staining for Flag or luciferase demonstrated strong, specific signals in the AAV9:hYAP and AAV9:Luci group, respectively (Online Figure IV-D,E). Together these data validate highly efficient AAV9-mediated YAP and luciferase expression in the heart.

AAV9:hYAP improved cardiac function and survival after MI.

We next evaluated the effect of AAV9:hYAP on outcome after MI. We induced MI and then injected virus directly into the myocardium at three positions along the margin of the ischemic area (Fig. 6A). Experimentally, this was best done immediately after MI rather than one week later. In a short-term study, we administered EdU 4 days after MI and analyzed hearts 1 day later for viral expression and CM proliferation. In a long-term study, we followed the MI mice for 23 weeks to determine if AAV9:hYAP treatment increased survival after MI. An additional control group (Ctrl) was un-operated and received no AAV. By 5 days after MI and AAV9 delivery, AAV9:hYAP drove elevated expression of YAP (Fig. 6B). AAV9 is known to establish expression of its cargo for more than several months[15]. We confirmed sustained expression of our AAV9 constructs by measuring luciferase activity 23 weeks after MI and AAV9:Luci delivery. As shown in Fig. 6C, the luciferase signal was robust in the hearts of AAV9:Luci-treated mice, but was undetectable in mice treated with AAV9:hYAP. Moreover, luciferase activity was only detected in the heart and not in liver, skeletal muscle, or other organs. These data demonstrated that direct myocardial injection of AAV9 with the TNT promoter successfully drove long-term overexpression of cargo genes specifically in the heart.

We determined the effect of AAV9:hYAP on murine survival after MI, since improved survival is a gold-standard metric of the efficacy of a therapeutic intervention for MI. Over a 23 week follow-up period, we found that AAV9:hYAP enhanced survival after MI compared to AAV-Luci ($P = 0.0327$, Fig. 6D). This indicated that AAV9:hYAP enhances outcome after MI.

To evaluate whether AAV9:hYAP improved survival by preserving ventricular function, we performed echocardiography on mice at 2 and 4 weeks, and cardiac MRI at the completion of the study at 23 weeks. At 2 and 4 weeks, MI hearts had significantly reduced systolic function compared to sham controls. At 2 weeks, the degree of cardiac dysfunction was comparable between AAV9:hYAP and AAV9:Luci treatment

groups (Fig. 6E). However, at 4 weeks the AAV9:hYAP-treated hearts had significantly better systolic function than AAV9:Luci controls (Fig. 6E). At 23 weeks, cardiac MRI showed that systolic function of both groups was depressed and was not significantly different between the surviving 3 AAV9:Luci mice and 6 AAV9:hYAP mice, as assessed by ejection fraction and LV end systolic volume (LVESV; Fig. 6F). The difference between the 2-4 week echo data and the 23 week MRI data is likely to be due to survival bias, i.e. the mice with the lowest ejection fraction were likely to have died prior to 23 weeks and thereby masked differences between groups when examined at the time of cardiac MRI. This conclusion was supported by subgroup analysis of the 4 week echo data: mice that died between 4 and 23 weeks had significantly reduced heart function compared to mice that survived to 23 weeks (Fig. 6G). Overall, the data point to better preservation of heart function in AAV9:hYAP treated mice at early time points, with loss of this difference at late time points, likely due to survival bias.

YAP is an oncogene, and its activation in liver caused liver tumors[10, 11]. AAV9 is reported to transduce mainly heart, skeletal muscle and liver,[14] leading to the possibility that AAV9:hYAP might induce liver tumors. As shown in Fig. 6C, AAV9:Luci signal was only detected in the heart, likely due to direct myocardial injection and our use of the cardiac specific TNT promoter. To more fully exclude AAV9:hYAP induced liver tumors, we examined livers from AAV9:Luci and AAV9:hYAP treated mice. The gross morphology and liver weight of AAV9-treated livers was indistinguishable from sham controls (Online Figure V-A,B). Moreover, liver sections stained with HE showed no difference among three groups (Online Figure V-C). These data indicate that myocardial injection of AAV9:hYAP is not oncogenic, at least within the 23 week time frame of the study.

AAV9:hYAP induced CM proliferation without affecting CM apoptosis.

Since YAP regulates organ size by both promoting cell proliferation and suppressing cell death[10], we hypothesized that YAP activation after MI protects the heart through the same mechanisms. We tested this hypothesis by measuring cell proliferation and cell death in the hearts collected from the short-term study, i.e. 5 days after MI and myocardial delivery of viral vector. We measured the fraction of CMs that passed through S-phase during the EdU pulse that was administered 4 days after MI. In un-operated controls, EdU^+ CMs were very rare. In the border zone of MI mice, there were significantly more EdU^+ CMs in the AAV9:hYAP group than in the AAV9:Luci group (arrow, Fig. 7A-B; arrowheads indicate non-myocytes).

To investigate the effect of AAV9:hYAP on CM death, we used TUNEL and TNNI3 co-staining to measure the frequency of apoptotic CMs in the infarct border region. Apoptotic CMs were more frequent after MI compared to un-operated control, although their overall frequency was low, consistent with published data[16] (Fig. 7C-D). There was no significant difference in apoptotic CM frequency between AAV9:hYAP and AAV9:Luci groups.

The pro-proliferative activity of YAP requires its interaction with TEAD transcription factors[5]. Mutation of human Yap serine 94 to alanine blocks YAP interaction with TEAD and abolishes its proliferative activity.[5] To determine if TEAD interaction and YAP mitogenic activity are essential for YAP preservation of function in the MI-injured heart, we generated AAV9-YAP[S94A;S127A] (abbreviated AAV9:hYAPS94A) and compared it to AAV9:hYAP. One month after MI and AAV delivery, AAV9:hYAP and AAV9:hYAPS94A drove equivalent levels of YAP expression (Online Figure VI-A). AAV9:hYAP–transduced hearts showed higher fractional shortening and lower heart weight to body weight ratio than AAV9:Luci control, consistent with our results reported above. However, AAV9:hYAPS94A–transduced mice were not distinguishable from AAV:Luci controls (Online Figure VI-B,C). Furthermore, AAV9:hYAP but not AAV9:hYAPS94A–treated mice had more EdU^+ CMs than the AAV9:Luci control (Online Figure VI-D,E). These data together suggest that YAP-TEAD interaction and YAP mitogenic activity is required for preserving heart function after MI.

Transcriptional profiling highlights biological processes modulated by AAV9:hYAP.

To gain greater understanding of the effect of YAP on myocardial injury responses, we performed genome-wide transcriptional profiling. Five days after MI and AAV injection, we collected heart apexes for microarray analysis (Fig. 8A). Compared with AAV9:Luci group, 774 genes and 350 genes were down- and up-regulated in the AAV9:hYAP group, respectively ($P<0.05$; Fold-change > 0.5 $\log_2$ scale; Online Table III and Fig. 8B). Genes up-regulated by YAP were related to cell cycle regulation, wound healing, and inflammation (Fig. 8C). Down-regulated genes were enriched for functional terms related to cardiomyopathy, heart development, and myofibril assembly. Interestingly, the other major category of functional terms enriched for down-regulated genes was related to energy metabolism, tricarboxylic acid cycle, and hexose metabolic processes. We chose several differentially expressed genes from these categories for validation by qRT-PCR. Overall the agreement between microarray and qRT-PCR was excellent. Compared to MI+AAV9:Luci, the MI+AAV9:hYAP group had higher expression of genes linked the inflammation (*Ccl2*, *Ccl7*, *Mmp8*, *Il1b*) and cell cycle regulation (*Aurka*, *Ccnb1*, *Ccna2*, *Cdc20*, *Cdk1*), and lower expression of genes related to sarcomeres (*Mybpc3*, *Myh6*, *Myh7*, and *Myl3*) (Fig. 8D).

Prolonged myocardial inflammation after MI contributes to adverse myocardial remodeling[17]. For example, upregulation of the inflammatory marker IL6 was a predictor of adverse myocardial outcome after MI[18]. To determine if YAP effect on myocardial inflammatory markers was transient or sustained, we measured expression of eight inflammatory marker genes one month after MI, including *Ccl2*, *Ccl7*, *Mmp8*, and *Il1b*, which were upregulated by AAV:YAP at 5 days after MI compared to AAV:Luci (Fig. 8D). These 4 inflammatory marker genes, as well as additional markers *Icam1*, *Il10*, and *Tgfb1*, were expressed at comparable levels between AAV:YAP and AAV:Luci at one month, suggesting resolution of the effect observed at 5 days (Fig. 8E). Expression of *Il6* was significantly downregulated by AAV:YAP (Fig. 8E), consistent with the beneficial effect of AAV:YAP on myocardial wound healing.

Overall, our data show that Yap promotes a less mature myocardial gene expression profile with reduced expression of sarcomere and oxidative phosphorylation genes, and increased expression of cell cycle genes. YAP enhanced the inflammatory response shortly after MI, but this response was short-lived and resolves by one month.

DISCUSSION

The mammalian heart's limited innate regenerative capacity, the vulnerability of the heart to myocardial insults, and the inadequacies of current heart disease treatment have led to a search for approaches to enhance adult heart regeneration. Enticing adult mammalian CMs to re-enter the cell cycle productively has proven to be a tremendous challenge,[8] and approaches that increase or sustain fetal or neonatal CM proliferation have often failed to translate to the adult mammalian heart.[19, 20] Thus, approaches initially developed in model systems based on CMs that have not terminally exited the cell cycle, such as adult zebrafish or fetal or neonatal mouse, need to be critically assessed in an adult mammalian system.

The Hippo-YAP pathway is a critical regulator of organ size, and YAP activation through either YAP overexpression or Hippo loss-of-function enhances cell proliferation.[1] Based on these data, we and others studied Hippo-YAP regulation of heart growth, and showed that YAP robustly stimulates CM proliferation in fetal and newborn heart.[3-5] In the current study, we induced YAP expression in adult CMs using two independent methods (inducible, CM-specific transgene and cardiac-specific AAV), and found that YAP promotes adult CM cell cycle re-entry. Moreover, we showed that YAP activation in the heart is well tolerated for up to three months and does not induce CM hypertrophy. After MI, YAP activation reduced scar size, improved heart function, and robustly enhanced survival.

While this study was in preparation, two manuscripts were published that reported on Hippo-YAP and postnatal heart regeneration. Olson and colleagues reported that constitutive overexpression of activated YAP enhanced neonatal heart regeneration, and that constitutive YAP activation reduced scarring and enhanced heart function after MI in 1 month old mice.[21] Martin and colleagues studied postnatal inactivation of Hippo kinase components *Salv* and *Lats1/2*.[22] One role of *Salv* and *Lats1/2* is to inhibit YAP; however, these genes also regulate a number of other CM responses, including hypertrophy, apoptosis, and autophagy.[23-25] Adult-stage knockout of these genes stimulated CM proliferation, and adult-stage *Salv* knockout commencing one week prior to MI improved heart function and reduced scar size at 3 weeks post-MI.[22] Our study is consistent with the pro-regenerative effects of YAP activation and advances the field by clearly showing that YAP drives CM cell cycle re-entry (as opposed to maintenance of a fetal proliferative state). Furthermore, we establish the long-term survival benefit of YAP activation. Critical for potential therapeutic translation, we further show that YAP retains efficacy when activated at the time of, or even one week after, myocardial infarction.

We used transcriptional profiling to define major biological processes influenced by YAP activation after MI. Interestingly, upregulated genes were enriched for functional annotations related inflammatory responses and wound healing. There is growing evidence that inflammatory responses play a complex role in myocardial injury responses. While aspects of sustained myocardial inflammation adversely affect myocardial outcome after MI[17, 26], inflammatory responses are also essential for regenerative responses, including mammalian heart regeneration[27, 28]. Our finding that YAP regulates wound healing is consistent with a recent report showing that YAP is essential for skin wound healing.[29] YAP acutely upregulated inflammation genes, with expression normalizing by one month after MI. It will be interesting to assess whether this transiently enhanced inflammatory response is contributes to or detracts from the overall beneficial activity of YAP.

Our data also suggest that YAP promotes a CM transcriptional profile notable for downregulation of muscle and oxidative metabolism genes characteristic of mature CMs, and upregulation of cell cycle genes. This transcriptional signature suggests that YAP activation may promote a less mature CM state conducive to proliferation.[30] YAP regulation of mitochondrial structure and function is intimately linked to its regulation of proliferation,[31] suggesting a potential direct link between YAP activation, mitochondrial gene expression, and proliferation in the heart. Sarcomere disassembly has been suggested to be integral to CM proliferation.[7] YAP induced downregulation of sarcomere genes such as *Myh6*, *Myh7*, *Mybpc3*, and *Myl3*, and this downregulation might contribute to YAP stimulation of CM proliferation. However, YAP-induced sarcomere gene downregulation appears to be selective to the context of MI, as we did not observe it in cultured neonatal rat CMs.[5] Further studies will be required to decipher how YAP coordinates regulation of genes related to muscle, metabolism, and proliferation.

Measurement of CM proliferation is a difficult challenge.[8] Measurement of the fraction of CMs in S phase (EdU) or M phase (pH3) can overestimate the extent of new CM formation, because CMs can become polyploidy or multinucleated. It has been suggested that measurement of Aurora B kinase provides additional specificity by marking cells undergoing cytokinesis,[32] but it is necessary to distinguish the subset of Aurora B^+ cells with staining localized to the cleavage furrow (and therefore undergoing cytokinesis) from nuclear staining observed throughout mitosis. This distinction is difficult and subjective in tissue sections. Previously, a multi-color fluorescent reporter was used to study the clonal origins of the zebrafish heart,[33] and another group used the cluster size of a sparsely activated monochromatic reporter to measure CM proliferation in response to an exogenous agent.[7] Here, we combined these strategies and coupled sparse Cre activation of a Dox-inducible transgene with Cre activation of a multi-color reporter. This assay provided an independent method to measure productive, transgene-stimulated CM proliferation. Because some Cre-labeled cells may not overexpress YAP, this method may underestimate the extent of proliferation. However, the observation that single color, multi-cell CM clusters are more frequent in YAP^{GOF} while dual

color multi-cell clusters are not provides clear evidence that YAP stimulates productive CM proliferation. Furthermore, this method provides evidence that YAP's mitogenic activity is cell autonomous.

Adult YAP activation drove modest levels of CM proliferation, while fetal YAP activation robustly augmented CM proliferation. This likely accounts for the modest beneficial effect of YAP on heart function and fibrosis after MI. Why is YAP mitogenic activity reduced in adult CMs? Potentially, changes in YAP protein-protein interactions in the adult heart might reduce its transcriptional activity. For instance, alpha-catenin and plakoglobin are strongly expressed in adult heart, and YAP interaction with these factors [34, 35] at cell-cell junctions may reduce its transcriptional potency (even when phosphorylation is inhibited by mutation of the Hippo kinase site). Alternatively, the well-known general block to adult CM proliferation may pose a non-specific impediment to YAP-stimulated proliferation.

In conclusion, we demonstrated that YAP activation in the adult heart is well tolerated. We showed that YAP activation after MI improves cardiac function and survival, providing proof of concept that YAP or its downstream targets have therapeutic efficacy in improving outcome after MI. YAP stimulates CM proliferation and modulates myocardial inflammatory responses, and these effects likely contribute to its efficacy in improving outcome after MI.

ACKNOWLEDGEMENTS

We thank David Bennett at Small Animal Imaging Core in the Beth Israel Deaconess Medical Center for collecting the MRI data. We thank Vionnie Yu and David Scadden for sharing the CAG-fs-RFP mouse prior to publication. The authors are grateful to R.J. van der Geest (Leiden University Medical Centre, Leiden) for providing the Mass software for the analysis of the MRI data.

SOURCES OF FUNDING

Z.L. was supported by an AHA postdoctoral fellowship. W.T.P. was supported by NIH HL116461 and HL100401, by an AHA Established Investigator Award, and by charitable contributions from Gail Federici Smith, Edward Marram, and Karen Carpenter.

DISCLOSURES

The authors have no conflicts of interest to disclose.

REFERENCES

1. Zhao B, Li L, Lei Q, Guan KL. The Hippo-YAP pathway in organ size control and tumorigenesis: an updated version. *Genes Dev*. 2010;24:862-874.
2. Zhao B, Ye X, Yu J, Li L, Li W, Li S, Yu J, Lin JD, Wang CY, Chinnaiyan AM, Lai ZC, Guan KL. TEAD mediates YAP-dependent gene induction and growth control. *Genes Dev*. 2008;22:1962-1971.
3. Heallen T, Zhang M, Wang J, Bonilla-Claudio M, Klysik E, Johnson RL, Martin JF. Hippo pathway inhibits Wnt signaling to restrain cardiomyocyte proliferation and heart size. *Science*. 2011;332:458-461.
4. Xin M, Kim Y, Sutherland LB, Qi X, McAnally J, Schwartz RJ, Richardson JA, Bassel-Duby R, Olson EN. Regulation of insulin-like growth factor signaling by Yap governs cardiomyocyte proliferation and embryonic heart size. *Sci Signal*. 2011;4:ra70.
5. von Gise A, Lin Z, Schlegelmilch K, Honor LB, Pan GM, Buck JN, Ma Q, Ishiwata T, Zhou B, Camargo FD, Pu WT. YAP1, the nuclear target of Hippo signaling, stimulates heart growth through cardiomyocyte proliferation but not hypertrophy. *Proc Natl Acad Sci U S A*. 2012;109:2394-2399.
6. Grieger JC, Choi VW, Samulski RJ. Production and characterization of adeno-associated viral vectors. *Nat Protoc*. 2006;1:1412-1428.
7. Bersell K, Arab S, Haring B, Kuhn B. Neuregulin1/ErbB4 signaling induces cardiomyocyte proliferation and repair of heart injury. *Cell*. 2009;138:257-270.
8. Zhou B, Lin Z, Pu WT. Mammalian Myocardial Regeneration. In: Hill JA, Olson E, eds. *Muscle: Fundamental Biology and Mechanisms of Disease*. Elsevier; 2012:555-569.
9. Snippert HJ, van der Flier LG, Sato T, van Es JH, van den Born M, Kroon-Veenboer C, Barker N, Klein AM, van Rheenen J, Simons BD, Clevers H. Intestinal crypt homeostasis results from neutral competition between symmetrically dividing Lgr5 stem cells. *Cell*. 2010;143:134-144.
10. Dong J, Feldmann G, Huang J, Wu S, Zhang N, Comerford SA, Gayyed MF, Anders RA, Maitra A, Pan D. Elucidation of a universal size-control mechanism in Drosophila and mammals. *Cell*. 2007;130:1120-1133.
11. Camargo FD, Gokhale S, Johnnidis JB, Fu D, Bell GW, Jaenisch R, Brummelkamp TR. YAP1 increases organ size and expands undifferentiated progenitor cells. *Curr Biol*. 2007;17:2054-2060.
12. Pasumarthi KB, Nakajima H, Nakajima HO, Soonpaa MH, Field LJ. Targeted expression of cyclin D2 results in cardiomyocyte DNA synthesis and infarct regression in transgenic mice. *Circ Res*. 2005;96:110-118.
13. Daya S, Berns KI. Gene therapy using adeno-associated virus vectors. *Clin Microbiol Rev*. 2008;21:583-593.
14. Zincarelli C, Soltys S, Rengo G, Rabinowitz JE. Analysis of AAV serotypes 1-9 mediated gene expression and tropism in mice after systemic injection. *Mol Ther*. 2008;16:1073-1080.
15. Kaspar BK, Roth DM, Lai NC, Drumm JD, Erickson DA, McKirnan MD, Hammond HK. Myocardial gene transfer and long-term expression following intracoronary delivery of adeno-associated virus. *J Gene Med*. 2005;7:316-324.
16. Knaapen MW, Davies MJ, De Bie M, Haven AJ, Martinet W, Kockx MM. Apoptotic versus autophagic cell death in heart failure. *Cardiovasc Res*. 2001;51:304-312.
17. Christia P, Frangogiannis NG. Targeting inflammatory pathways in myocardial infarction. *European Journal of Clinical Investigation Eur J Clin Invest*. 2013;43:986-995.
18. Gabriel AS, Martinsson A, Wretlind B, Ahnve S. IL-6 levels in acute and post myocardial infarction: their relation to CRP levels, infarction size, left ventricular systolic function, and heart failure. *European Journal of Internal Medicine*. 2004;15:523-528.
19. Oh H, Taffet GE, Youker KA, Entman ML, Overbeek PA, Michael LH, Schneider MD. Telomerase reverse transcriptase promotes cardiac muscle cell proliferation, hypertrophy, and survival. *Proc Natl Acad Sci U S A*. 2001;98:10308-10313.

20. Novoyatleva T, Diehl F, van Amerongen MJ, Patra C, Ferrazzi F, Bellazzi R, Engel FB. TWEAK is a positive regulator of cardiomyocyte proliferation. *Cardiovasc Res*. 2010;85:681-690.
21. Xin M, Kim Y, Sutherland LB, Murakami M, Qi X, McAnally J, Porrello ER, Mahmoud AI, Tan W, Shelton JM, Richardson JA, Sadek HA, Bassel-Duby R, Olson EN. Hippo pathway effector Yap promotes cardiac regeneration. *Proc Natl Acad Sci U S A*. 2013;110:13839-13844.
22. Heallen T, Morikawa Y, Leach J, Tao G, Willerson JT, Johnson RL, Martin JF. Hippo signaling impedes adult heart regeneration. *Development*. 2013;140:4683-4690.
23. Matsui Y, Nakano N, Shao D, Gao S, Luo W, Hong C, Zhai P, Holle E, Yu X, Yabuta N, Tao W, Wagner T, Nojima H, Sadoshima J. Lats2 is a negative regulator of myocyte size in the heart. *Circ Res*. 2008;103:1309-1318.
24. Maejima Y, Kyoi S, Zhai P, Liu T, Li H, Ivessa A, Sciarretta S, Del Re DP, Zablocki DK, Hsu CP, Lim DS, Isobe M, Sadoshima J. Mst1 inhibits autophagy by promoting the interaction between Beclin1 and Bcl-2. *Nat Med*. 2013;19:1478-1488.
25. Yamamoto S, Yang G, Zablocki D, Liu J, Hong C, Kim SJ, Soler S, Odashima M, Thaisz J, Yehia G, Molina CA, Yatani A, Vatner DE, Vatner SF, Sadoshima J. Activation of Mst1 causes dilated cardiomyopathy by stimulating apoptosis without compensatory ventricular myocyte hypertrophy. *J Clin Invest*. 2003;111:1463-1474.
26. Huang GN, Thatcher JE, McAnally J, Kong Y, Qi X, Tan W, DiMaio JM, Amatruda JF, Gerard RD, Hill JA, Bassel-Duby R, Olson EN. C/EBP Transcription Factors Mediate Epicardial Activation During Heart Development and Injury. *Science*. 2012;338:1599-1603.
27. Godwin JW, Pinto AR, Rosenthal NA. Macrophages are required for adult salamander limb regeneration. *Proc Natl Acad Sci U S A*. 2013
28. Aurora AB, Porrello ER, Tan W, Mahmoud AI, Hill JA, Bassel-Duby R, Sadek HA, Olson EN. Macrophages are required for neonatal heart regeneration. *The Journal of Clinical Investigation J Clin Invest*. 2014;124:1382-1392.
29. Lee MJ, Ran Byun M, Furutani-Seiki M, Hong JH, Jung HS. YAP and TAZ Regulate Skin Wound Healing. *J Invest Dermatol*. 2014;134:518-525.
30. Szibor M, Poling J, Warnecke H, Kubin T, Braun T. Remodeling and dedifferentiation of adult cardiomyocytes during disease and regeneration. *Cell Mol Life Sci*. 2013
31. Nagaraj R, Gururaja-Rao S, Jones KT, Slattery M, Negre N, Braas D, Christofk H, White KP, Mann R, Banerjee U. Control of mitochondrial structure and function by the Yorkie/YAP oncogenic pathway. *Genes Dev*. 2012;26:2027-2037.
32. Engel FB, Schebesta M, Keating MT. Anillin localization defect in cardiomyocyte binucleation. *J Mol Cell Cardiol*. 2006;41:601-612.
33. Gupta V, Poss KD. Clonally dominant cardiomyocytes direct heart morphogenesis. *Nature*. 2012;484:479-484.
34. Chen SN, Gurha P, Lombardi R, Ruggiero A, Willerson JT, Marian AJ. The hippo pathway is activated and is a causal mechanism for adipogenesis in arrhythmogenic cardiomyopathy. *Circ Res*. 2014;114:454-468.
35. Schlegelmilch K, Mohseni M, Kirak O, Pruszak J, Rodriguez JR, Zhou D, Kreger BT, Vasioukhin V, Avruch J, Brummelkamp TR, Camargo FD. Yap1 acts downstream of alpha-catenin to control epidermal proliferation. *Cell*. 2011;144:782-795.

FIGURE LEGENDS

Figure 1. Cardiac phenotype of YAP^{GOF} mice. A. Dox-regulated, CM-specific expression system. **B.** Cardiac YAP expression of Dox-treated mice was measured by western blot. **C.** RT-PCR showing YAP overexpression in YAP^{GOF} heart. **D.** Dox-dependent YAP expression in YAP^{GOF} mice.

Figure 2. YAP stimulates adult CM proliferation. YAP^{GOF} and control mice were treated with Dox from 4 to 8 weeks of life. Hearts were analyzed at 8 weeks. **A.** Heart weight to body weight ratio was not significantly different between groups. **B-C.** CM cross-sectional area was lower in YAP^{GOF} than in control. WGA-stained sections were used to measure CM cross-sectional area. n=6-7. Bar = 25 μm. **D.** The relative number of CMs in YAP^{GOF} and control hearts based on heart weight and CM cross-sectional area. *, P< 0.05. **E-G.** The size and number of CMs isolated from hearts by collagenase perfusion. n=4-8. Bar = 50 μm. **H-I.** The fraction of CMs bearing proliferative markers EdU or pH3 was determined in dissociated heart preparations. Yellow arrow indicates proliferating CM, and arrowhead indicates a non-myocyte. n=5. Bar = 25 μm. **J.** Nucleation of all CMs compared to EdU^{+} CMs was determined in dissociated cardiomyocytes. The large majority of proliferating CMs in control and YAP^{GOF} groups were mononuclear.

Figure 3. Clonal analysis of YAP-induced adult CM proliferation. A-C. One color clonal analysis of CM proliferation. (A), Schematic of the experimental design. * indicates adjacent cells that were labeled by two separate recombination events, rather than by proliferation of a single labeled cell. (B), Representative images. Red arrows indicate a cluster of three red cells. (C), Quantification showing that clusters of 2 or more RFP^{+} cells were found more frequently in YAP^{GOF} hearts. n=5 hearts per group. Bar = 50 μm or 10 μm. **D-F.** Two color clonal analysis of CM proliferation. (D), experimental design. * indicates a bichromatic cluster caused by two independent labeling events. (E), Representative images. Yellow arrows, bichromatic clusters. Red arrows, monochromatic clusters. The number of arrows sharing a common tail indicates the number of cells in that cluster. (F). Quantification showing that monochromatic clusters with ≥ 2 cells were more common in YAP^{GOF}. Bichromatic clusters were not significantly different between groups. n=4 hearts per group. Bar = 25 μm.

Figure 4. Cardiac specific overexpression of YAP is well tolerated in adult mouse. Cardiac specific overexpression of YAP is well tolerated in adult mouse. **A-B.** 4 months of YAP induction in adult heart did not grossly affect heart size, morphology (A), or HW/BW ratio (B). A, bar=5 mm. **C-D.** Echocardiographic analysis of prolonged YAP overexpression on adult heart function. LVPW;d, diastolic left ventricular posterior wall thickness. *, P<0.05. n=4. **E-F.** Effect of YAP overexpression on myocardial fibrosis, assessed by picosirius red/fast green staining. (E), Representative sections. Fibrotic areas stain red. (F), Quantification. NS, not significant.

Figure 5. Activated YAP improved myocardial outcome after MI. A. Experimental design. **B-C.** MRI assessment of ventricular function. B, representative images. C, quantification. Bar = 5 mm. **D.** HW/BW was lower in YAP^{GOF}. **E-F.** Scar size, measured as a percentage of ventricular circumference in sequential picro-sirus red and fast green stained sections. Bar = 5 mm. **G.** EdU^{+} CMs were more frequent in YAP^{GOF} border and remote zones. Representative section shows an EdU^{+} CM (arrow) in YAPG^{OF}. Bar = 25 μm. H. pH3^{+} CMs were more frequent in YAP^{GOF}. Representative section shows a pH3^{+} CM (arrow). Bar = 10 μm.

Figure 6. Myocardial AAV9:hYAP injection post MI improved cardiac function and mouse survival. A. Schematic of AAV9:hYAP therapeutic trial on wild-type mice. **B.** YAP mRNA level measured by qRT-PCR on total RNA from the hearts collected in the short-term study. The YAP mRNA level was normalized to GAPDH. n=3. **C.** Bioluminescent imaging. 23 weeks after MI, AAV9:hYAP and AAV9:Luci groups were examined for luciferase activity. **D.** Kaplan Meier survival analysis. AAV9:Luci, n=10, AAV9:hYAP, n=7. **E.** Heart function measured by echocardiography at 2 weeks and 4 weeks after MI. FS, fractional

shortening. Sham, n=3, AAV9:Luci (Luci), n=9, AAV9:hYAP (YAP), n=7. **F.** Heart function measured by MRI at 23 weeks after MI. EF, Ejection fraction, LVESV, left ventricular end systolic volume. AAV9:Luci, n=3, AAV9:hYAP, n=6. G. Between 4 and 23 weeks after MI, 6 AAV:Luci animals died of heart failure and 3 survived. Heart function at 4 weeks after MI was compared between survivors and non-survivors.

Figure 7. AAV9:hYAP increased CM proliferation. Cell proliferation was measured by uptake of a pulse of EdU given 4 days after MI and AAV delivery. Hearts were analyzed one day after EdU administration. **A-B.** Cardiomyocyte proliferation was measured by EdU update. Arrowheads indicate non-CMs, and arrow indicates CMs. *, $P<0.05$. **C.** Cardiomyocyte apoptosis was measured by TUNEL staining. **D.** Quantification of $TUNEL^+$ CMs. NS, not significant. n=3 for each group. Bar = 100 μm.

Figure 8. Biological processes perturbed by YAP activation. A. Experimental design. 5 days after MI and AAV9:hYAP or AAV9:Luci injection, total RNA was prepared from heart apex. **B.** Differentially expressed genes (FC > 0.5 in $\log_2$ scale; $P < 0.05$) segregated samples by treatment group. **C.** GO term enrichment analysis of up- and down-regulated genes. All GO terms in "Biological Processes_FAT" or KEGG Pathways with Benjamini-Hochberg p < 1.0E-4 are shown, after removing closely related terms. **D.** qRTPCR validation of microarray gene expression measurements. **E**. qRT-PCR measurement of inflammation genes one month after MI and AAV injection. *, $P<0.05$.

Novelty and Significance

What Is Known?

- Reduced cardiac myocyte (CM) number underlies many forms of heart failure. Therapeutic approaches that stimulate CM proliferation would be immensely beneficial.
- The evolutionarily conserved Hippo-YAP pathway critically regulates organ growth and has been shown to stimulate fetal and neonatal CM proliferation.
- Constitutive YAP activation from fetal through adult stages sustains CM cell cycle activity, enhances neonatal and juvenile heart regeneration, and attenuates cardiac dysfunction after MI.
- Whether or not induced expression of YAP stimulates cell cycle re-entry of adult, terminally differentiated CMs, and the efficacy of therapeutic YAP activation in the adult heart shortly after myocardial infarction, are largely unknown.

What New Information Does This Article Contribute?

- YAP activation in the heart did not cause cardiac hypertrophy and was well tolerated for three months.
- Activation of YAP in adult CMs, driven either by adult-stage activation of a cardiac-restricted transgene or by a CM-selective AAV9 vector, stimulates CM proliferation.
- Activation of YAP in adult CMs after myocardial infarction attenuates cardiac dysfunction and improves long-term survival.
- YAP activation after MI upregulates genes related to inflammation and cell cycle, and downregulates genes related to oxidative metabolism and muscle cells.
- Mosaic transgene activation in CMs labeled with a multicolor fluorescent reporter is an effective method to test the transgene's cell autonomous stimulation of CM proliferation.

In an effort to address the tremendous biomedical need for approaches to enhance the limited innate regenerative capacity of the mammalian heart, we studied the effect of YAP activation in the adult heart. Our results show that sustained YAP activation is well tolerated in the heart, and that YAP drives productive adult CM proliferation. Furthermore, YAP activation shortly after myocardial infarction improved myocardial function and survival. Thus, activation of YAP or its downstream targets should be further evaluated as regenerative approaches to heart disease.

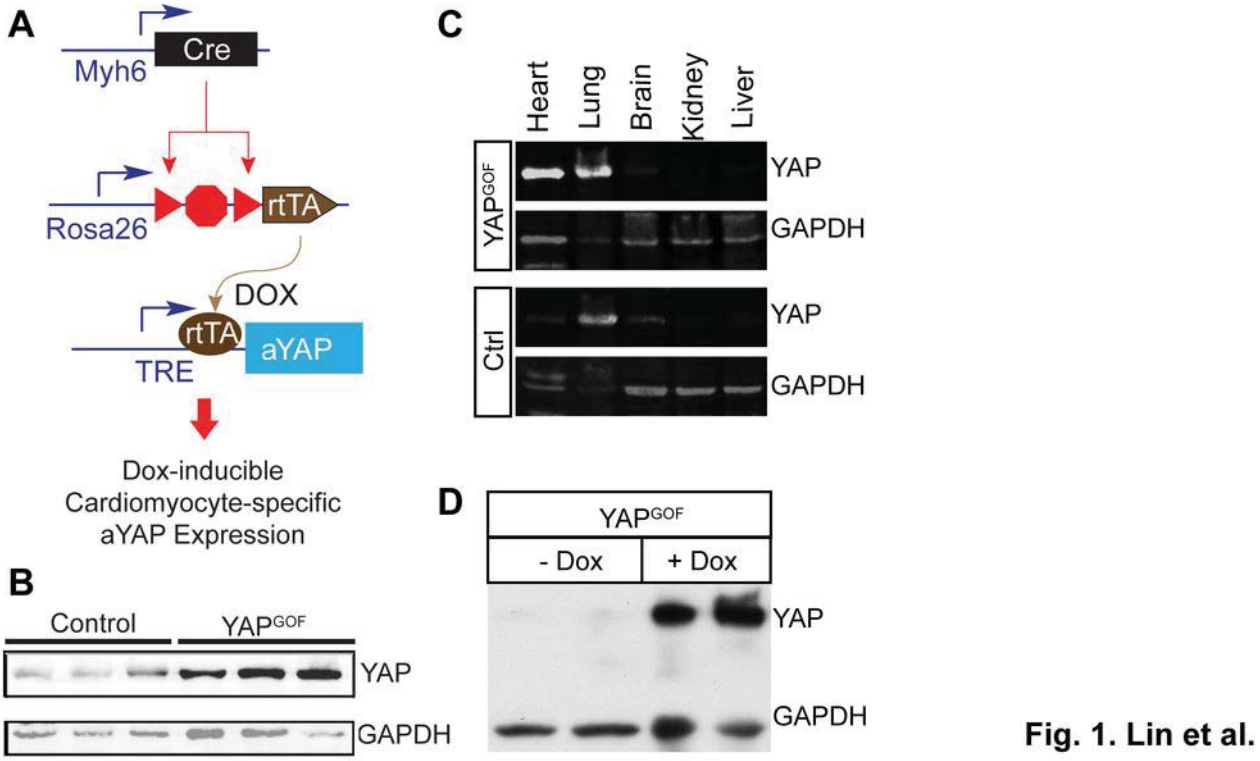

Fig. 1. Lin et al.

Figure 1. Cardiac phenotype of YAP^{GOF} mice. A. Dox-regulated, cardiomyocyte-specific expression system. **B.** Cardiac YAP expression of Dox-treated mice was measured by western blot. **C.** YAP was selectively overexpressed in YAP^{GOF} heart. **D.** Dox-dependent YAP expression in YAP^{GOF} hearts.

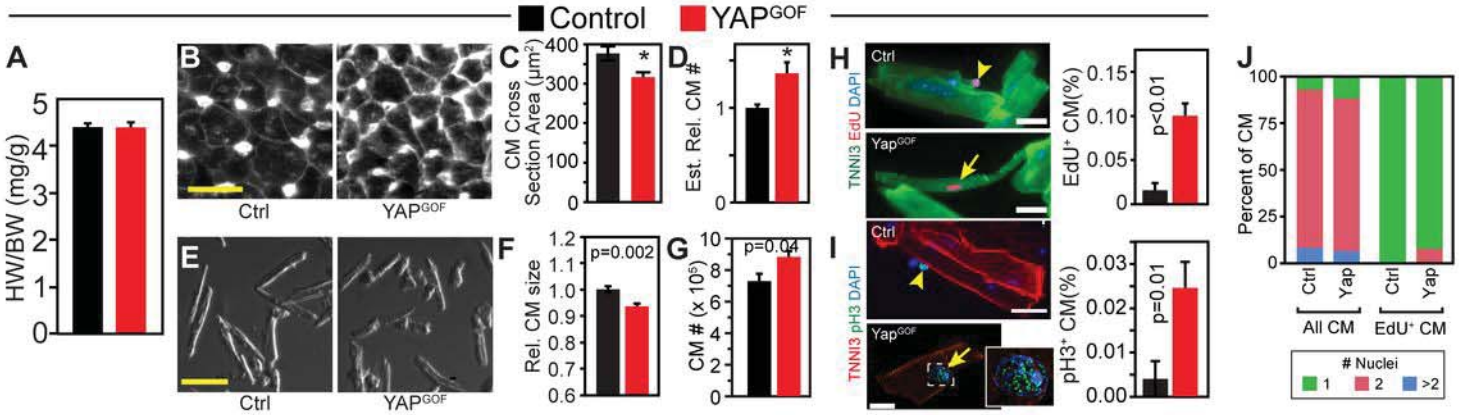

Fig. 2. Lin et al.

YAP stimulates adult CM proliferation. YAP^{GOF} and control mice were treated with Dox from 4 to 8 weeks of life. Hearts were analyzed at 8 weeks. **A.** Heart weight to body weight ratio was not significantly different between groups. **B-C.** CM cross-sectional area was lower in YAPGOF than in control. WGA-stained sections were used to measure CM cross-sectional area. n=6-7. Bar = 25 μm. **D.** The relative number of CMs in YAP^{GOF} and control hearts based on heart weight and CM cross-sectional area. **E-G.** The size and number of CMs isolated from hearts by collagenase perfusion. n=4-8. Bar = 50 μm. **H-I.** The fraction of CMs bearing proliferative markers EdU or pH3 was determined in dissociated heart preparations. Yellow arrow indicates proliferating CM, and arrowhead indicates a non-myocyte. n=5. Bar = 25 μm. **J.** Nucleation of all CMs compared to EdU^{+} CMs was determined in dissociated cardiomyocytes. The large majority of proliferating CMs in control and YAPGOF groups were mononuclear. *, P< 0.05.

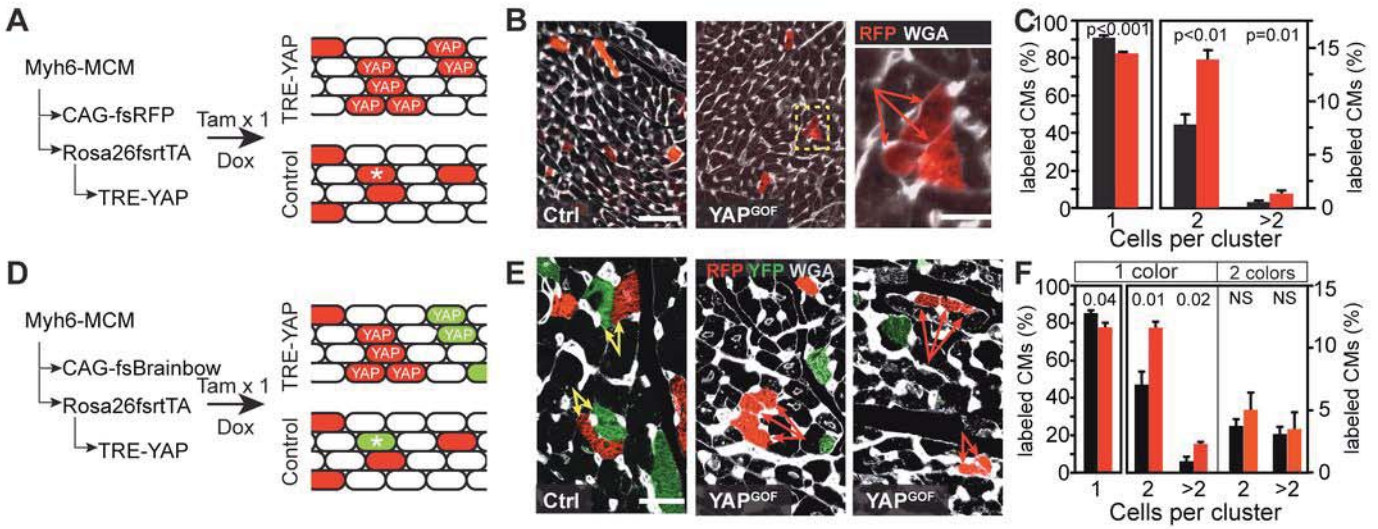

Figure 3. Lin et al.

Figure 3. Clonal analysis of YAP-induced adult CM proliferation. A-C. One color clonal analysis of CM proliferation. (A), Schematic of the experimental design. * indicates adjacent cells that were labeled by two separate recombination events, rather than by proliferation of a single labeled cell. (B), Representative images. Red arrows indicate a cluster of three red cells. (C), Quantification showing that clusters of 2 or more RFP^{+} cells were found more frequently in YAP^{GOF} hearts. n=5 hearts per group. Bar = 50 μm or 10 μm. **D-F.** Two color clonal analysis of CM proliferation. (D), experimental design. * indicates a bichromatic cluster caused by two independent labeling events. (E), Representative images. Yellow arrows, bichromatic clusters. Red arrows, monochromatic clusters. The number of arrows sharing a common tail indicates the number of cells in that cluster. (F). Quantification showing that monochromatic clusters with ≥ 2 cells were more common in YAP^{GOF}. Bichromatic clusters were not significantly different between groups. n=4 hearts per group. Bar = 25 μm.

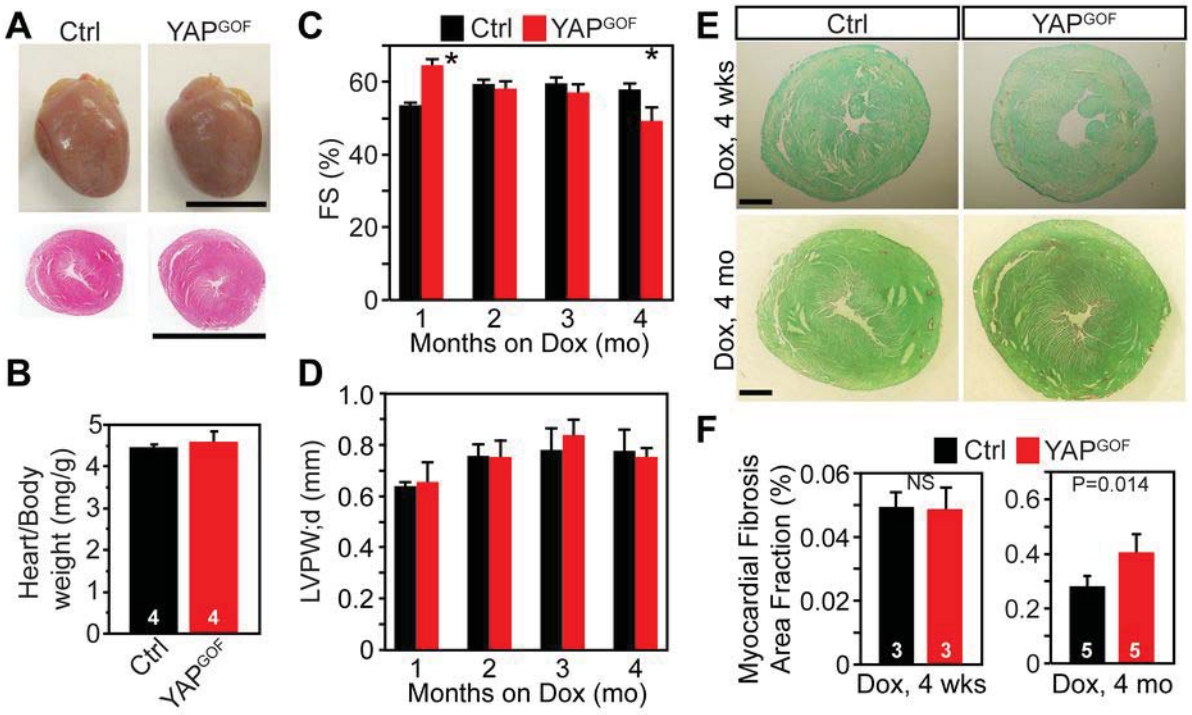

Figure 4. Lin et al.

Cardiac specific overexpression of YAP is well tolerated in adult mouse. **A-B.** 4 months of YAP induction in adult heart did not grossly affect heart size, morphology (A), or HW/BW ratio (B). A, bar=5 mm. **C-D.** Echocardiographic analysis of prolonged YAP overexpression on adult heart function. LVPW;d, diastolic left ventricular posterior wall thickness. *, P<0.05. n=4. **E-F.** Effect of YAP overexpression on myocardial fibrosis, assessed by picosirius red/fast green staining. (E), Representative sections. Fibrotic areas stain red. (F), Quantification. NS, not significant.

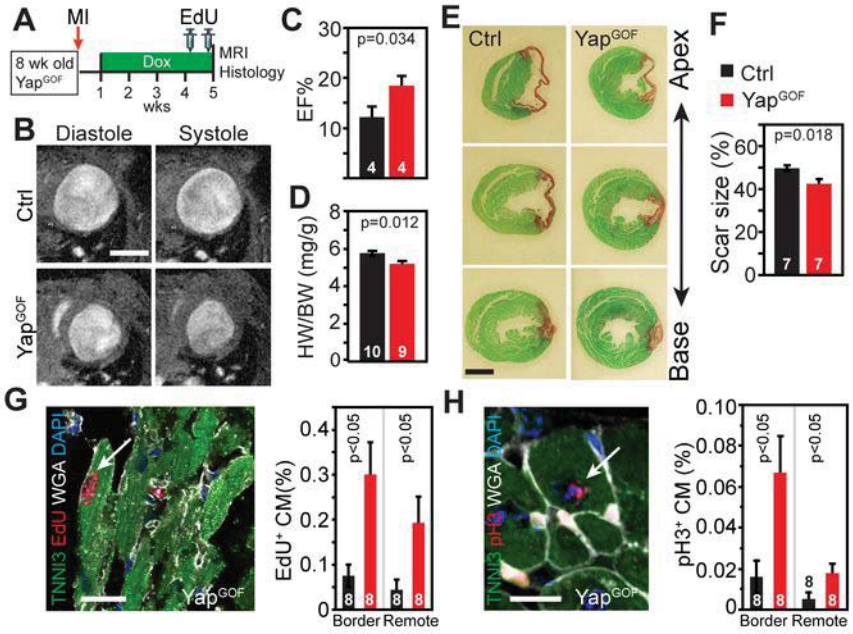

Fig. 5. Lin et al.

Activated YAP improved myocardial outcome after MI. A. Experimental design. **B-C.** MRI assessment of ventricular function. B, representative images. C, quantification. Bar = 5 mm. **D.** HW/BW was lower in YAP^{GOF}. **E-F.** Scar size, measured as a percentage of ventricular circumference in sequential picro-sirus red and fast green stained sections. Bar = 5 mm. **G.** EdU^{+} CMs were more frequent in YAP^{GOF} border and remote zones. Representative section shows an EdU^{+} CM (arrow) in YAP^{GOF}. Bar = 25 μm. **H.** pH3^{+} CMs were more frequent in YAP^{GOF}. Representative section shows a pH3^{+} CM (arrow). Bar = 10 μm.

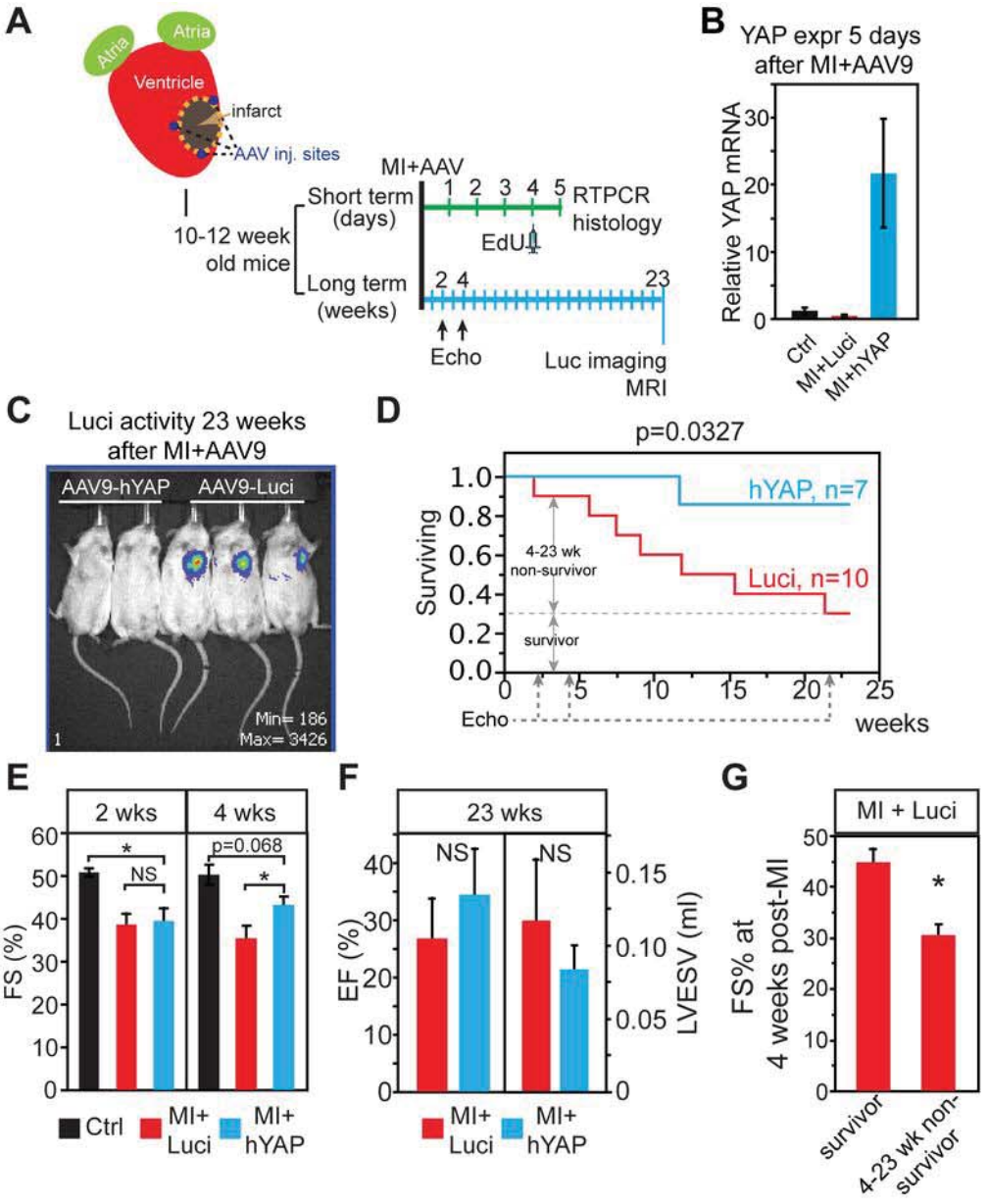

Figure 6. Lin et al.

Myocardial AAV9:hYAP injection post MI improved cardiac function and mouse survival. A. Schematic of AAV9:hYAP therapeutic trial on wild-type mice. **B.** YAP mRNA level measured by qRT-PCR on total RNA from the hearts collected in the short-term study. The YAP mRNA level was normalized to GAPDH. n=3. **C.** Bioluminescent imaging. 23 weeks after MI, AAV9:hYAP and AAV9:Luci groups were examined for luciferase activity. **D.** Kaplan Meier survival analysis. AAV9:Luci, n=10, AAV9:hYAP, n=7. **E.** Heart function measured by echocardiography at 2 weeks and 4 weeks after MI. FS, fractional shortening. Sham, n=3, AAV9:Luci (Luci), n=9, AAV9:hYAP (YAP), n=7. **F.** Heart function measured by MRI at 23 weeks after MI. EF, Ejection fraction, LVESV, left ventricular end systolic volume. AAV9:Luci, n=3, AAV9:hYAP, n=6. **G.** Between 4 and 23 weeks after MI, 6 AAV:Luci animals died of heart failure and 3 survived. Heart function at 4 weeks after MI was compared between survivors and non-survivors.

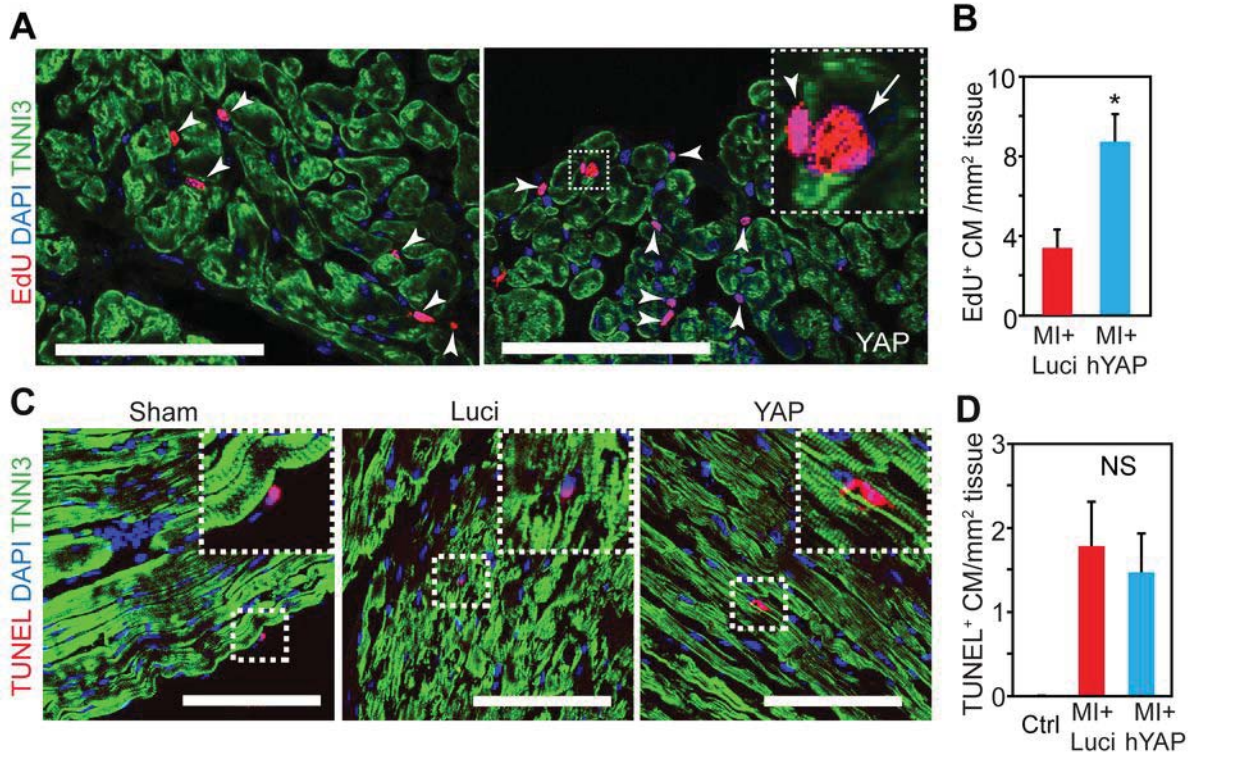

Figure 7. AAV9:hYAP increased cardiomyocyte proliferation. Cell proliferation was measured by uptake of a pulse of EdU given 4 days after MI and AAV delivery. Hearts were analyzed one day after EdU administration. **A-B.** A higher fraction of AAV9:hYAP CMs were EdU$^+$ than AAV9:Luci CMs. Arrowheads indicate non-cardiomyocytes, and arrow indicates cardiomyocyte. *, P<0.05. **C**. TUNEL$^+$ cardiomyocytes were found in MI + AAV groups, but not in the unoperated control group. The frequency of TUNEL$^+$ CMs was not significantly different between groups. **D.** Quantification of TUNEL$^+$ CMs did not show a significant difference between AAV9:Luci and AAV9:hYAP groups. n=3 for each group. Bar = 100 μm.

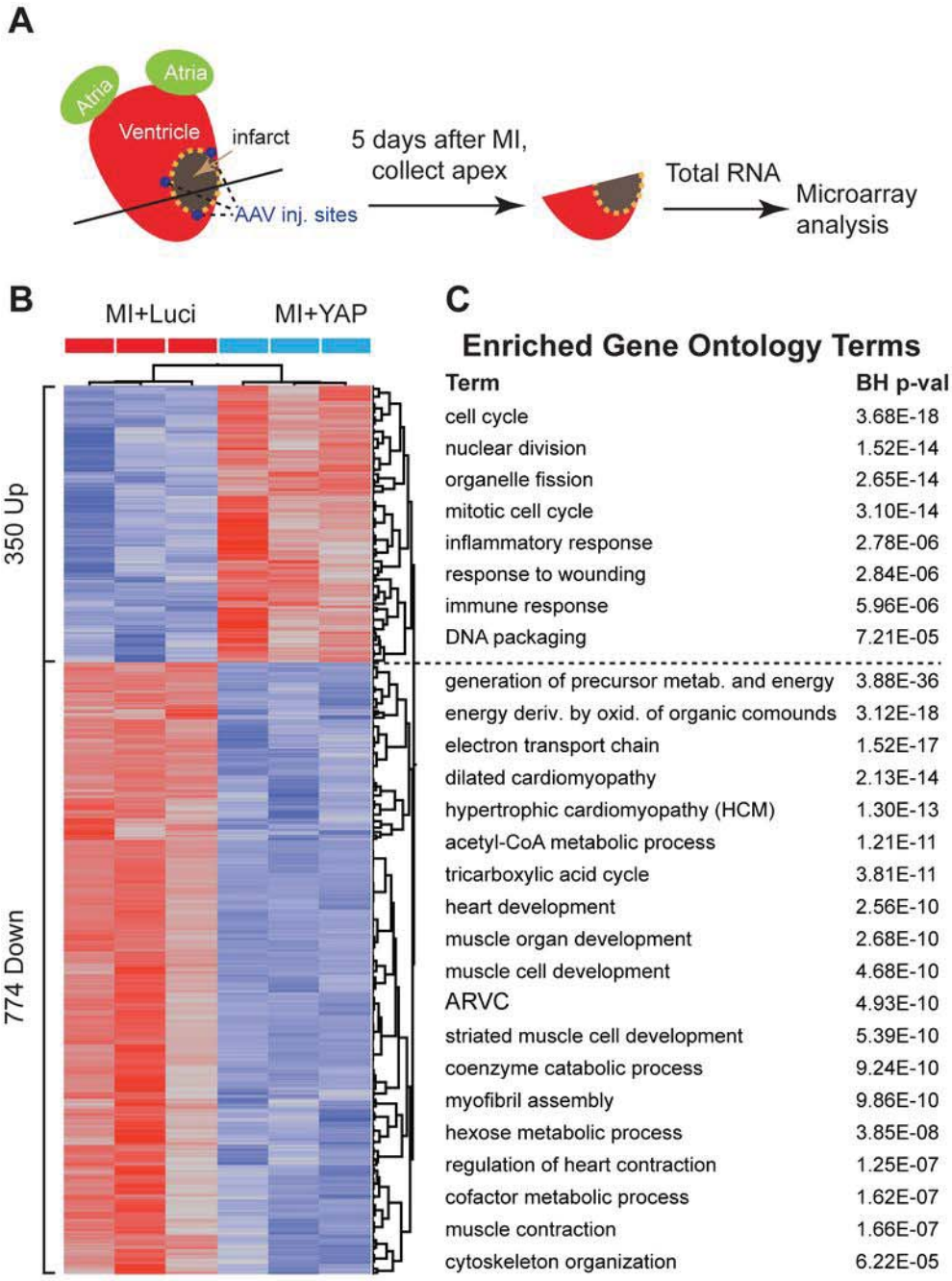

Figure 8. Biological processes perturbed by YAP activation. A. Experimental design. 5 days after MI and AAV9:hYAP or AAV9:Luci injection, total RNA was prepared from heart apex. **B.** Differentially expressed genes (FC > 0.5 in log2 scale; P < 0.05) segregated samples by treatment group. **C.** GO term enrichment analysis of up- and down-regulated genes. All GO terms in "Biological Processes_FAT" or KEGG Pathways with Benjamini-Hochberg p < 1.0E-4 are shown, after removing closely related terms. **D.** qRTPCR validation of microarray gene expression measurements. **E.** qRT-PCR measurement of inflammation genes one month after MI and AAV injection. *, P<0.05.

Supplemental Material, Lin et al.

Cardiac specific YAP activation post myocardium infarction improved cardiac function and mouse survival

A. Detailed Materials and Methods.

Animal experiments

All animal procedures were approved by the Institutional Animal Care and Use Committee. TetO-YAP[1], Rosa26$^{fs\text{-}rtTA2}$, and MHCα–Cre[3] alleles were previously described. Dox was administered at 1 mg/mL in drinking water. 5-ethynyl-2'deoxyuridine (EdU) was administered at 5 μg/g body weight IP. To induce MI, mice aged 8 weeks were subjected to LAD ligation as described previously.[4]

Echocardiography was performed on a VisualSonics Vevo 2100 with Vevostrain software. Magnetic resonance imaging (MRI) was carried out at Small Animal Imaging Core in Beth Israel Hospital. For in vivo bioluminescent imaging, mice were administered Luciferin (150 μg/gram body weight IP), sedated using isoflurane, and imaged 10 min later on a Xenogen IVIS System.

MI, echocardiography, and MRI were performed blinded to genotype and treatment group.

Immunohistochemistry.

Hearts were fixed and embedded in OCT. 8 μm cryosections were used for immunostaining, using antibodies listed in Online Table 1. EdU was detected with the Click-iT EdU imaging kit (Invitrogen). TUNEL staining was performed using the Roche in situ death detection kit. Imaging was performed on a Fluoview 1000 confocal microscope, or a Nikon TE2000 epifluorescent microscope.

AAV9 packaging

3Flag-hYAP and Luciferase were separately cloned into ITR-containing AAV plasmid (Penn Vector Core P1967) harboring the chicken cardiac TNT promoter, to get pAAV.cTnT::3Flag-hYAP and pAAV.cTnT::Luciferase, respectively. AAV9 was packaged in 293T cells with AAV9:Rep-Cap and pHelper (pAd deltaF6, Penn Vector Core) and purified and concentrated by gradient centrifugation[5]. AAV9 titer was determined by quantitative PCR.

Gene Expression

Real time PCR was performed with Syber Green or Taqman detection using an ABI 7500 thermocycler. PCR primers are listed in Online Table II. Expression profiling of total RNA from heart apex was performed using Affymetrix 2.0 ST microarrays. The microarray data is available at GSE57719 and tabulated in Online Table III. GO term analysis used DAVID.[6]

Infarct size measurement

Heart sections were collected at regular intervals. Sections were stained with Sirius Red-Fast Green. Digital images were captured and infarct sizes were calculated according to the formula: [infarct perimeter (epicardial +endocardial)/ total perimeter (epicardial + endocardial)] x 100.[7]

Statistics

Values are expressed as mean ± SEM. For two group comparisons, Student's t-test was used to test for statistical significance. To analyze data containing more than two groups, we used ANOVA with the Tukey HSD post-hoc test. Both tests were performed using JMP 10.0 (SAS).

B. Supplemental References

1. Camargo FD, Gokhale S, Johnnidis JB, Fu D, Bell GW, Jaenisch R, Brummelkamp TR. YAP1 increases organ size and expands undifferentiated progenitor cells. Curr Biol. 2007;17:2054-2060.
2. Belteki G, Haigh J, Kabacs N, Haigh K, Sison K, Costantini F, Whitsett J, Quaggin SE, Nagy A. Conditional and inducible transgene expression in mice through the combinatorial use of Cre-mediated recombination and tetracycline induction. Nucleic Acids Res. 2005;33:e51.
3. Agah R, Frenkel PA, French BA, Michael LH, Overbeek PA, Schneider MD. Gene recombination in postmitotic cells. Targeted expression of Cre recombinase provokes cardiac-restricted, site-specific rearrangement in adult ventricular muscle in vivo. J Clin Invest. 1997;100:169-179.

4. Tarnavski O, McMullen JR, Schinke M, Nie Q, Kong S, Izumo S. Mouse cardiac surgery: comprehensive techniques for the generation of mouse models of human diseases and their application for genomic studies. Physiol Genomics. 2004;16:349-360.
5. Grieger JC, Choi VW, Samulski RJ. Production and characterization of adeno-associated viral vectors. Nat Protoc. 2006;1:1412-1428.
6. Huang da W, Sherman BT, Lempicki RA. Systematic and integrative analysis of large gene lists using DAVID bioinformatics resources. Nat Protoc. 2009;4:44-57.
7. Pasumarthi KB, Nakajima H, Nakajima HO, Soonpaa MH, Field LJ. Targeted expression of cyclin D2 results in cardiomyocyte DNA synthesis and infarct regression in transgenic mice. Circ Res. 2005;96:110-118.

C. Online Tables

Online Table I. Antibodies used in this study

Primary antibodies			
Antigen	**Company**	**Origin**	**Working dilution**
Cardiac troponin I (TNNI3)	Abcam	Goat	1:200 for IF
Flag	Sigma	Rabbit	1:200 for IF
Luciferase	Abcam	Rabbit	1:200 for IF
488 phalloidin	IncPHDG1-A	NA	1:200 for IF
GAPDH	Sigma	Mouse	1:200,000 for WB
Cardiac Myosin Heavy chain	Abcam	Mouse	1:200 for IF
WGA-555	Invitrogen	NA	1:250 for IF
YAP	Sigma	Rabbit	1:1000 for WB
Secondary antibodies			
Anti-Goat Alexa488	Invitrogen	Donkey	1:500 for IF
Anti-Goat Alexa647	Invitrogen	Donkey	1:500 for IF
Anti-Rabbit Alexa555	Invitrogen	Donkey	1:500 for IF
Anti-Rabbit HRP	Invitrogen	Goat	1:10,000 for WB

Online Table II. Primers Used in This Study

Primers		
Gene*	**Forward**	**Reverse**
m/hYAP	*GACCCTCGTTTTGCCATGA*	*ATTGTTCTCAATTCCTGAGAC*
mCCNA2	GCCTTCACCATTCATGTGGAT	TTGCTCCGGGTAAAGAGACAG
mCDK1	TTTCGGCCTTGCCAGAGCGTT	GTGGAGTAGCGAGCCGAGCC
mCCNB1	AAGGTGCCTGTGTGTGAACC	GTCAGCCCCATCATCTGCG
mCDC20	TTCGTGTTCGAGAGCGATTTG	ACCTTGGAACTAGATTTGCCAG
mAurka	GGGTGGTCGGTGCATGCTCCA	GCCTCGAAAGGAGGCATCCCCACTA
mCCL2	GTTGGCTCAGCCAGATGCA	AGCCTACTCATTGGGATCATCTTG
mCCL7	AGAAGCAAGGCCAGCACAGAGT	GAGCAGCAGGCACAGAAGCGT
mMMP8	AATCCTTGCCCATGCCTTTCAACC	CCAAATTCATGAGCAGCCACGAGA
mIl6	CACTTCACAAGTCGGAGGCT	CTGCAAGTGCATCATCGTTGT
mICAM	CAGTCCGCTGTGCTTTGAGA	AGGGTGAGGTCCTTGCCTAC
mIl10	GGTGAGAAGCTGAAGACCCTC	GCCTTGTAGACACCTTGGTCTT
mTgfb1	ACTGGAGTTGTACGGCAGTG	TCATGTCATGGATGGTGCCC
mIL1B	TGTGCAAGTGTCTGAAGCAGCTA	TCAAAGGTTTGGAAGCAGCCCT
mMyh6	CTCTGGATTGGTCTCCCAGC	GTCATTCTGTCACTCAAACTCTGG
mMybpc3	CTGTCCATGAGGCCATTGGT	GCTTTGAGTCCCTCCGGAAA
mMyom1	TGGGTACTACATCGAGGCCA	GAGACACTCCTCCCCCGATA
mMyl3	CCAAAAAGCCAGAGCCCAAG	GGCCTCCTTGAACTCTTCAATC
ABI Taqman assays		
Gene*		
mGAPDH	4352339E	
Myh7	Mm00600555_m1	

*m=mouse; h=human

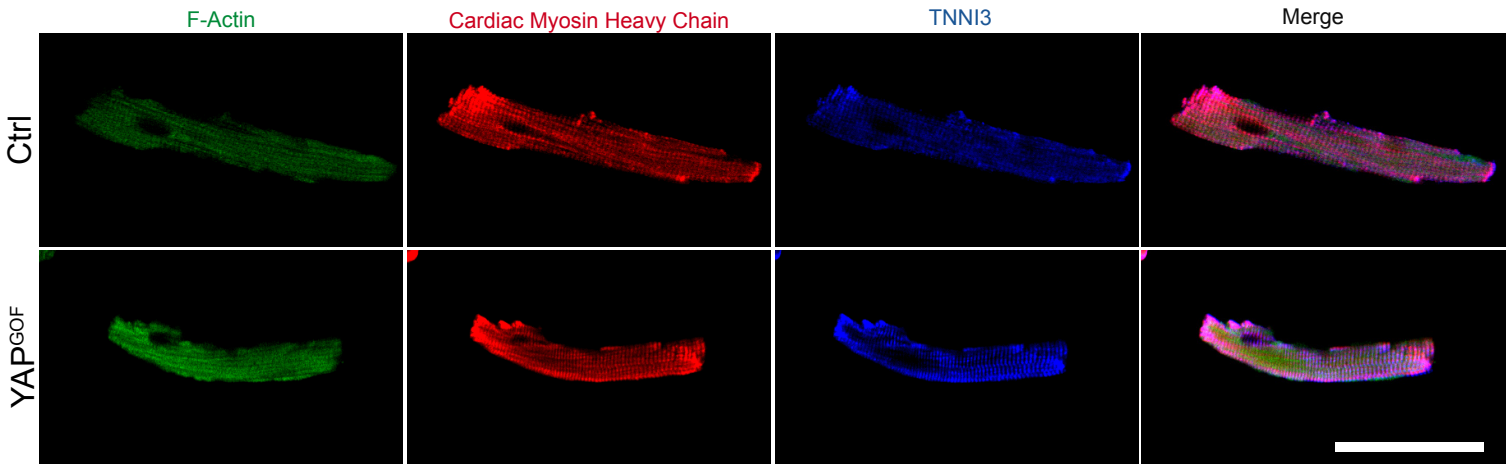

Online Figure I. Lin et al.
Representative images of sarcomere morphology of cardiomyocytes isolated from adult control and YAP^{GOF} hearts. Filamentous actin was stained with phalloidin. Cardiac myosin heavy chain antibody recognized both α and β isoforms. No difference in sarcomere organization was observed between treatment groups. Bar=50 μm

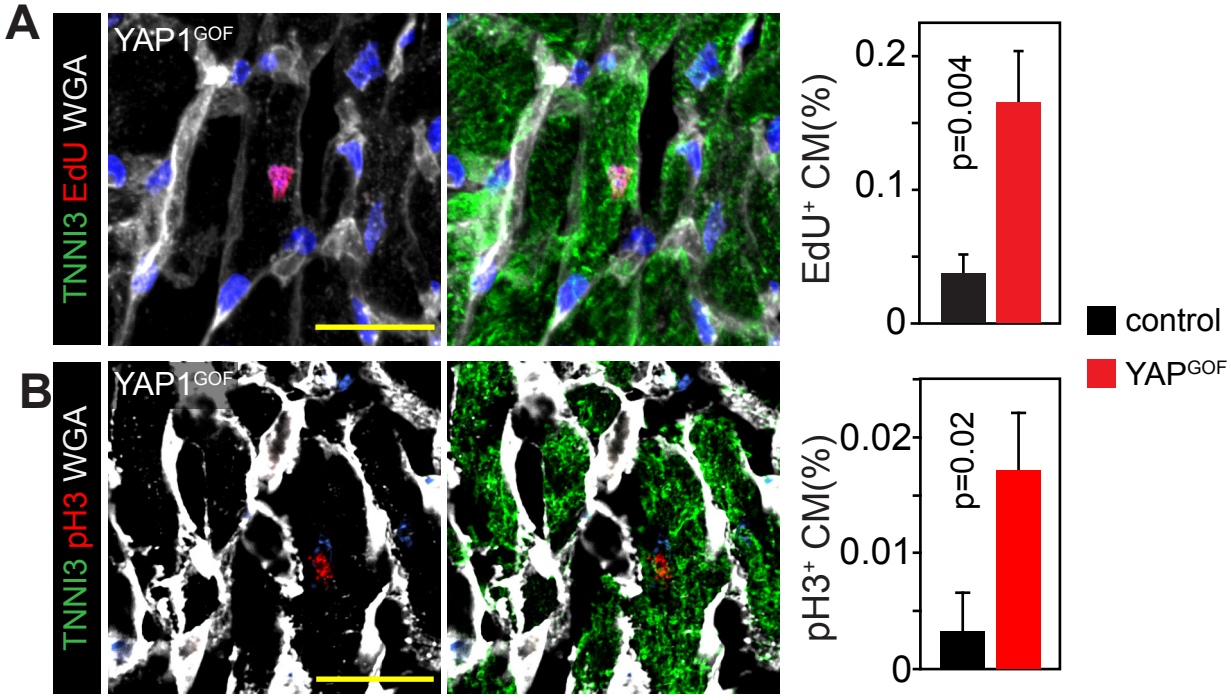

Online Figure II. Lin et al.
Cardiomyocyte cell cycle activity induced by expression of activated YAP. After Dox-induced expression of activated YAP from weeks of life 4 to 8, hearts were analyzed for cell cycle markers.
A. The fraction of cardiomyocytes in S-phase was determined by measuring EdU uptake. At least 5000 CMs were sampled per heart. n=6. Bar = 25 μm.
B. The fraction of cardiomyocytes in M-phase was determined by immunostaining for phosphohistone H3 (pH3). YAP increased the fraction of CMs in M-phase. At least 8000 CMs were sampled per heart. n=6. Bar = 25 μm.

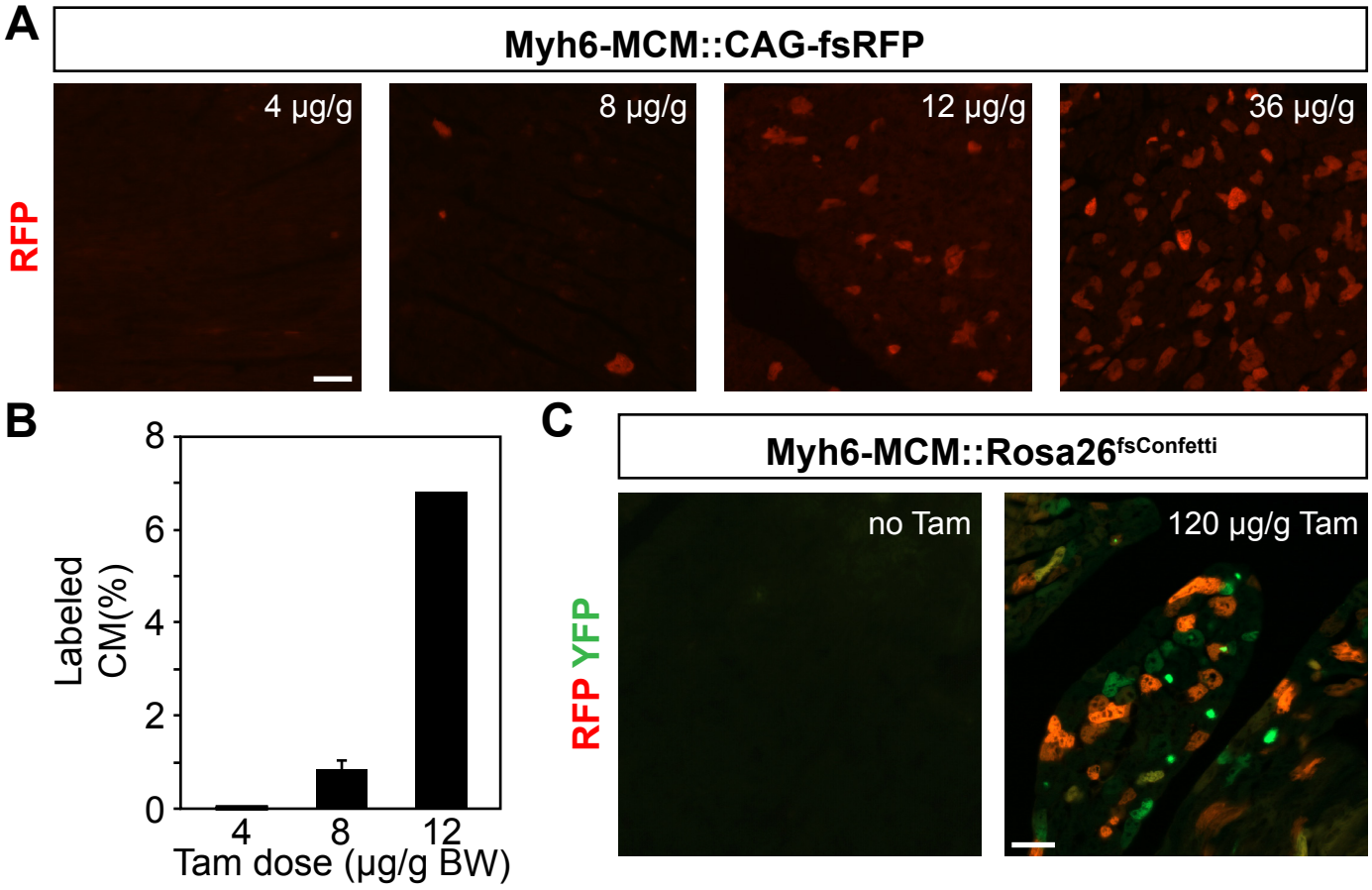

Online Figure III. Lin et al.
Tamoxifen titration to achieve infrequent cardiomyocyte labeling by Myh6-MerCreMer.
A-B. The indicated dose of tamoxifen was administered to Myh6-MCM; CAG-fs-RFP mice. We measured the frequency of labeled cardiomyocytes (B).
C. Tamoxifen-induced activation of RFP or YFP from the Rosa26^{fsConfetti} reporter. Bar, 40 µm.

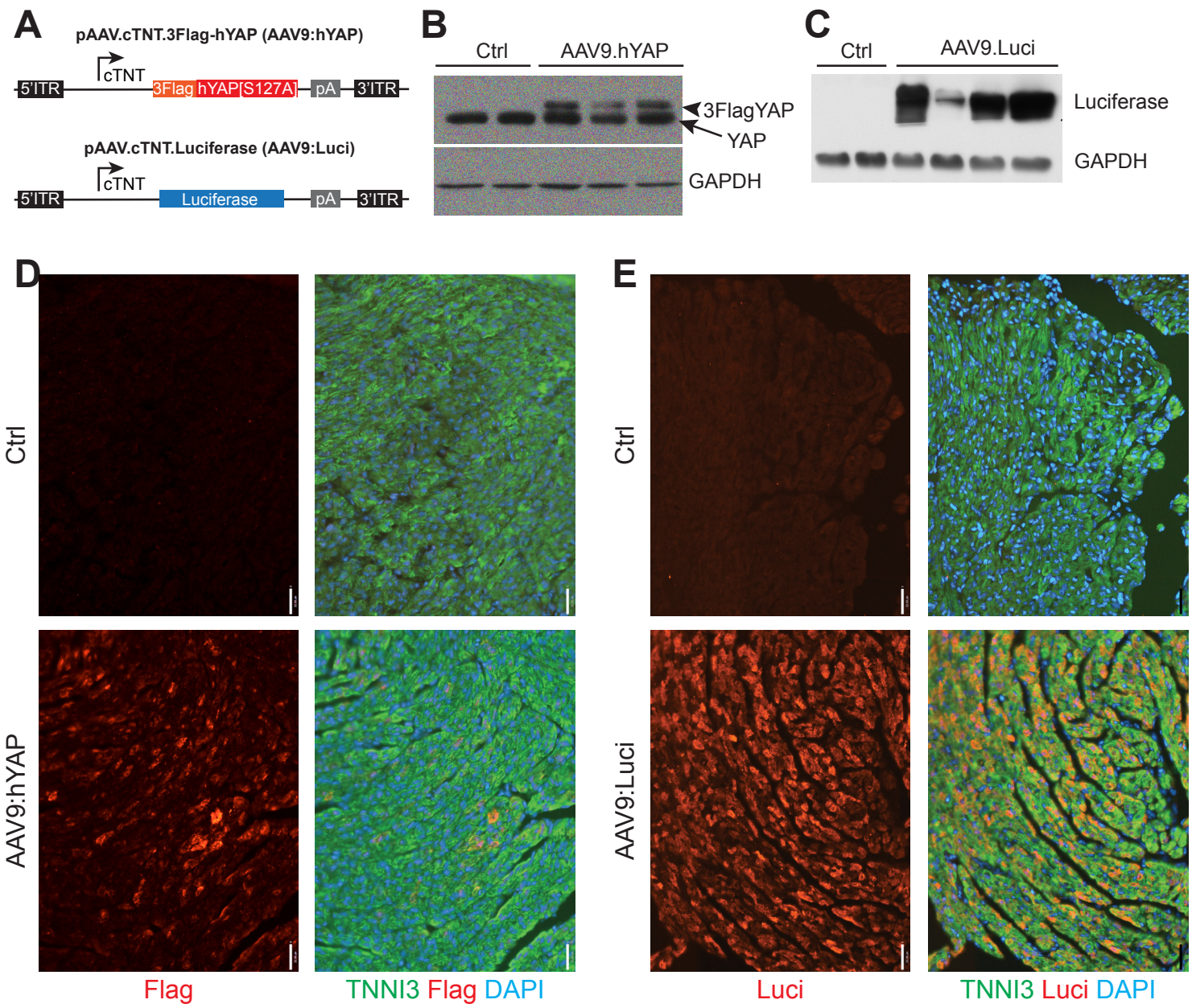

Online Figure IV. Lin et al.
AAV construction and validation.
A. AAV vectors used to generate AAV9:hYAP and AAV9:Luci contained the AAV inverted terminal repeats (ITRs), the chicken TNNT2 (cTNT) promoter, and a polyadenylation (pA) signal. 3Flag-hYAP[S127A] or luciferase were cloned into this AAV backbone to generate pAAV.cTNT.3Flag-hYAP (AAV9:hYAP) or pAAV.cTNT.Luciferase (AAV9:Luci), respectively.
B-C. AAV9:hYAP or AAV9:Luci viruses were injected subcutaneously into 3 day old mice . 5 days later, hearts were analyzed by western blotting. Mice that received no AAV9 injection served as control (Ctrl). Expression of 3Flag-hYAP (B, indicated by arrowhead) and Luciferase (C) was confirmed with western blot.
D. AAV9:hYAP expressed Flag-tagged YAP in the heart. Bar = 50 μm.
E. AAV9:Luci expressed luciferase in the heart. Bar = 50 μm.

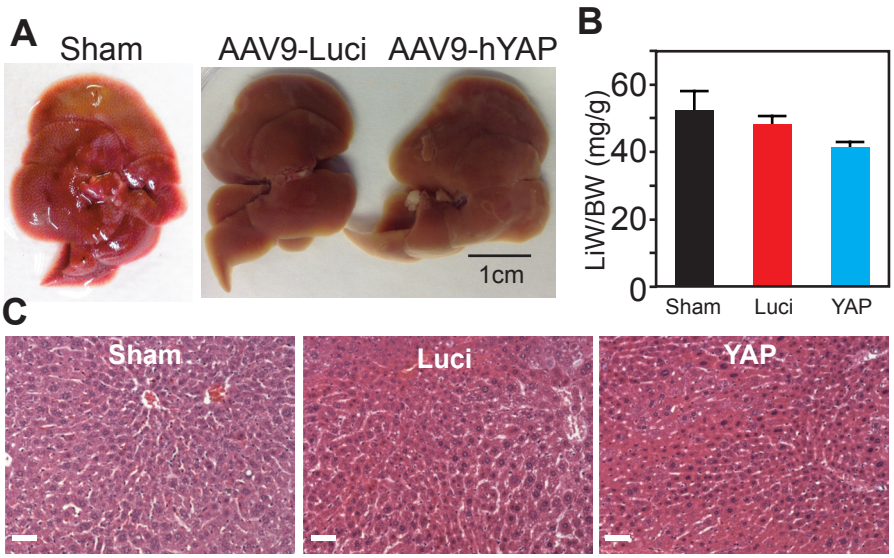

Online Figure V. Lin et al.
Direct intramyocardial injection of AAV9-hYAP did not cause liver tumors.
A. Gross morphology of livers from sham control, AAV9-Luci and AAV9-hYAP.
B. AAV9-hYAP did not alter liver weight to body weight ratio (LiW/BW). No significant difference was found between groups. Sham, n=3; AAV9-Luci, n= 3; AAV9-hYAP, n=6.
C. HE staining of liver sections did not reveal any hepatic tumors. Bar = 50 μm.

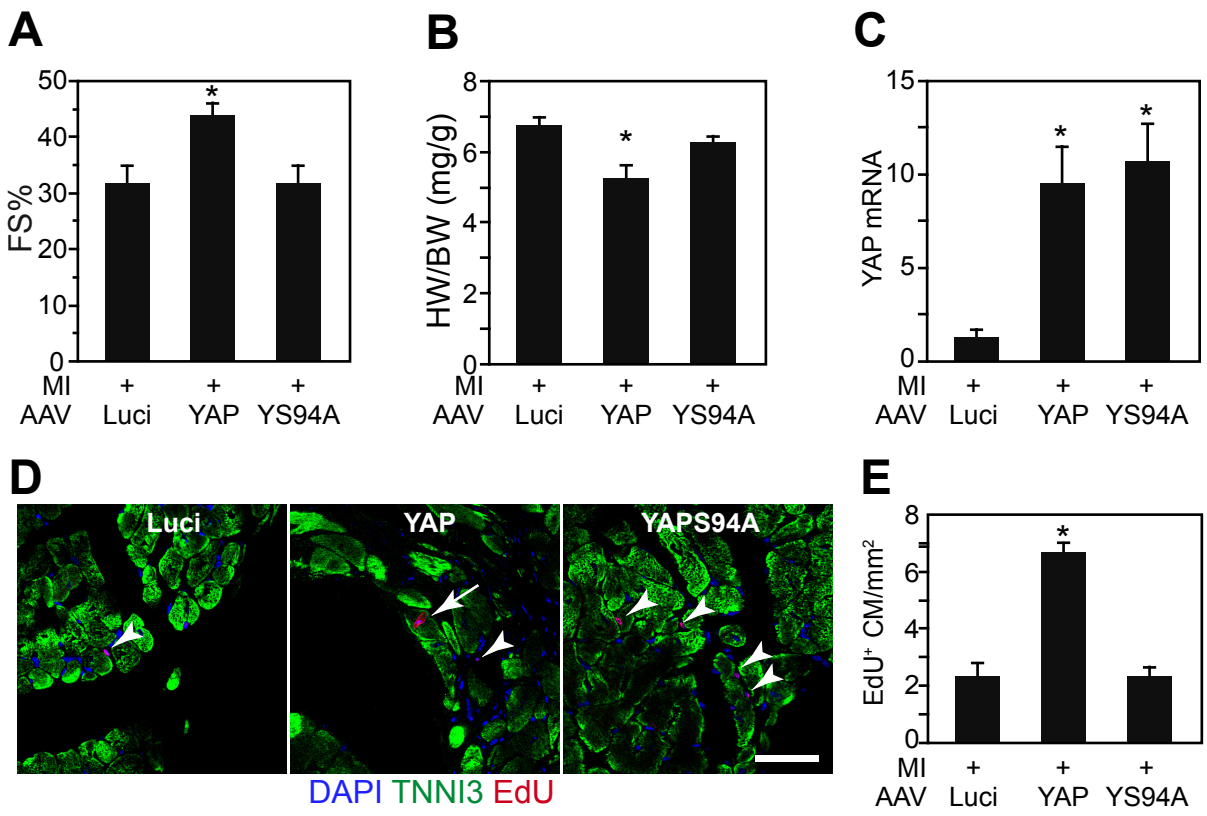

Online Figure VI, Lin et al.

YAP-TEAD interaction is required for beneficial activities of YAP after MI. Interaction of overexpressed YAP was abolished by mutation of serine 94 to alanine. Mice were treated with AAV9:YAP, AAV9:YAPS94A, or AAV9:Luci at the time of coronary artery ligation. Hearts were examined 1 month after MI.

A. Fraction shortening measured by echocardiography.

B. Heart weight to body weight ratio.

C. Total YAP mRNA level measured by qRT-PCR.

D-E. Cardiomyocyte proliferation assessed by EdU incorporation rate. EdU was administered in the fourth week after MI. White arrow heads indicate EdU positive non-cardiomyocytes. White arrow indicates EdU positive cardiomyocyte. Bar=50 μm.

*P<0.05. n=4